AAS-JAKOBSEN COWI Multiconsult

JOHS HOLT AkerSolutions entail NGI DISSING+WEITLING architecture a|s mossmaritime

Concept development, floating bridge E39 Bjørnafjorden

Appendix H – Enclosure 1

10205546-09-NOT-067
A simplified model to implement freeboard exceedance scenarios in OrcaFlex

MEMO

PROJECT	**Concept development, floating bridge E39 Bjørnafjorden**	DOCUMENT CODE	10205546-09-NOT-067
CLIENT	Statens vegvesen	ACCESSIBILITY	Restricted
SUBJECT	**A simplified model to implement freeboard exceedance scenarios in OrcaFlex**	PROJECT MANAGER	Svein Erik Jakobsen
CONTACT	Øyvind Kongsvik Nedrebø	PREPARED BY	Finn-Christian Wickmann Hanssen
		RESPONSIBLE UNIT	AMC

SUMMARY

A simplified model is proposed to account for freeboard exceedance on one or several pontoons in time domain. The physical phenomenon of freeboard exceedance is considered transient, and cannot be linearized for a frequency-domain analysis in a rational manner. The proposed model is based on existing models to estimate the effects of green water for ships and ship-shaped structures. This is based on a literature survey, investigating previous research in relevant fields.

Several assumptions are made in the model in order for it to be straightforward to implement. Most of these assumptions are believed to be conservative. The model can therefore not be expected to give fully accurate results, but is considered a useful mean to assess the consequences of freeboard exceedance.

Partly based on the performed literature survey, enhanced modelling strategies to be considered for later and more detailed phases of the project are briefly indicated.

1	29.03.2019	Status 2 issue	Finn-Christian W. Hanssen	Arnt G. Fredriksen	Svein Erik Jakobsen
0	19.02.2019	Issued for DNV GL review	Finn-Christian W. Hanssen	Arnt G. Fredriksen	Svein Erik Jakobsen
REV.	DATE	DESCRIPTION	PREPARED BY	CHECKED BY	APPROVED BY

0 Revision History

Revision	Changes
1	Errors in eqs. (4) and (7) corrected after DNV GL comments. Wave asymmetry factor changed from 1.1 to 1.2 based on DNV GL comments.
0	First issue.

1 Introduction

The present memo addresses numerical modelling of events involving full or partial exceedance of the freeboard capacity on one or more of the pontoons of the Bjørnafjorden floating bridge concept(s). When the freeboard exceedance is due to an amplified wave overtopping a pontoon, the involved physics are generally complex. At the present stage of the project, a general model that approximates the involved physical effects adequately, and that can be implemented in OrcaFlex in a straightforward manner is sought after. Such model is here proposed, with the intention to model the global effects on the system without having to adopt a local modelling for the detailed flow of water on top of the pontoon. Such model would be able to evolve the local shallow-water flow on deck in time, and thus provide a detailed description of the water height on deck and resulting fluid loads. The model proposed here is a qualitative one, and is hence not expected to be as accurate as solving the local flow-problem on top of the pontoon. However, assumptions believed to be conservative are made in the model, in order for it to represent a rational tool to investigate the possible consequences of freeboard exceedance.

Before proposing the model, a literature survey was performed. In general, it is found that waves overtopping a pontoon is analogue with the green-water phenomenon on ships and ship-shaped floaters. This problem has received considerable attention during the last decades, and is used as a basis to understand the involved physics and to get an overview of the numerical modelling techniques that have been proposed.

2 Previous Work

The main findings from the literature survey investigating previous relevant works are here presented. Few or none studies that focus directly on loss-of-freeboard events on surface-piercing pontoons have been found in the literature. However, the problem resembles that of green water/water on deck of ship-shaped units. This problem has been more frequently investigated over the past decades, and is here considered as a basis.

Bas Buchner's PhD thesis [1] represents a heavily cited work on green-water effects on ship-shaped structures. He investigated, both experimentally and numerically, the green-water phenomenon on ship bows with various shapes and flare angles. Here, the term "green water" is introduced to specify that there is a real amount of sea water on deck, and not just various types of spray. He gives a summary of previous relevant works, where a couple of notable observations are:

- The pressure in the water on deck is higher than the hydrostatic pressure in the water column on top of it, because also the vertical acceleration of the deck should be accounted for.
- According to the so-called "Glimm's method", the water flow on deck is a shallow-water flow that can be numerically simulated in a time-stepping scheme by discretizing the deck area into a grid.

The latter point is based on the fact that the depth-dependence disappears in shallow-water theories because the length scale in the problem is much larger than the vertical scale, so that the fluid velocity is assumed independent of the vertical axis. This method forms the basis for some of the other works that will be discussed, because it allows the water-on-deck and the global seakeeping problem to be

solved as a coupled system in time domain. Moreover, this approach reflects that the problem is a transient one due to the local flow of water on deck that depends on time-varying boundary conditions.

Buchner states that the relative motion between the structure and the wave can be seen as input to the green-water problem. From figures given in the thesis, it is found that green water loading can have a significant influence on the pitch motion of a ship. Buchner offers the following simplified model to estimate the pitch moment resulting from a green-water event, in which the deck is divided into N strips:

$$M(t) = \sum_{i=1}^{N} H_i(t)\rho\big(g + \ddot{z}_i(t)\big)l_i A_i, \tag{1}$$

Where $M(t)$ is the time-varying pitch moment due to the water on deck, $H_i(t)$ is the water-on-deck height in strip i, $\ddot{z}_i(t)$ is the vertical acceleration in strip i due to the floater motion, l_i is the strip's moment arm and A_i is the strip area. In his simplified study, Buchner took $H_i(t)$ from wave probe measurements in experiments. Buchner implemented equation (1) into the uncoupled equation of motion to demonstrate the effect on the pitch motion, i.e.

$$(I_{55} + A_{55})\ddot{\eta}_5 + B\dot{\eta}_5 + C\eta_5 = M_{wave}(t) + M(t), \tag{2}$$

where $M_{wave}(t)$ is the moment due to "standard" wave excitation.

Buchner states that the behaviour of the flow on deck in practice is influenced by the magnitude of the freeboard exceedance, the bow shape, the vessel motions and the wave period.

Buchner presented a simplified design evaluation method where some useful relations that may add to the physical interpretation of the problem:

- The water height on deck is given as $a_H h$, where h is the freeboard exceedance and a_H is a coefficient depending on the hull shape and distance from the bow given in Table 5-2 in [1]
- The fluid velocity on deck is estimate as $U = a_U\sqrt{H_0}$, where a_U is tabulated in Table 5-3 in [1] and H_0 is the water height on deck at the bow (fore perpendicular)
- The horizontal impact load on a structure on deck can be estimated as $F_x = a_F h^2$, with a_F given given in Table 6-2 in [1].

Greco & Lugni (2012) [2] coupled a weakly non-linear seakeeping code with a water-on-deck model based on shallow-water equations in 3D. This method can in principle be adopted in OrcaFlex, but is considered too complicated and time consuming for the present project phase. It is however to be taken into consideration when e.g. doing analysis towards the project end when a final concept is selected. Such novel methods should as a rule of thumb always be verified by dedicated model tests. Greco & Lugni demonstrate that their model gives a good description of how the water flows on deck, also when compared to CFD, as long as local effects such as fragmented flows are not of importance. They compared their model with experimental results for a patrol ship in head sea with and without forward speed that experienced water on deck in regular waves. In general, their study shows that water on deck may modify heave and pitch motions moderately, both in terms of amplitude and phase. The most dramatic effect is however related to horizontal impact loads on deckhouse structures. For the present project, with moderate wave heights, wave impact loads on the bridge columns are not considered as a dimensioning load case.

Wan et al. (2017) [3] used the water-on-deck model from [2] combined with a non-linear station keeping code (as is OrcaFlex) to study a combined wave energy converter and wind turbine. This had a shape that resembles that of the Bjørnafjorden pontoon, consisting of a circular pontoon with an upright wind column supporting the horizontal-axis wind turbine. The structure was floating, and the freeboard was in the same order of magnitude as in the present study. The combined model gave good comparison with model tests, confirming that such modelling approach indeed is attractive.

This is especially because it is much more computationally efficient than e.g. CFD methods. However, as already discussed, significant work goes into implementing such model.

3 Proposed Simplified Model for OrcaFlex at Present Stage

The main assumptions behind the proposed model are:

- Events where the freeboard is lost lead to transient type of loading that can only be considered in time domain. There is no rational manner in which such loading can be linearized in a frequency-domain model.
- Loss of freeboard is analouge to a water-on-deck problem, with shallow-water flow on deck and where the resulting fluid pressure is given by the hydrostatic pressure in the water column plus a term that is proportional to the vertical acceleration of the deck.

The latter point means that merely removing the water-plane restoring forces and moments does not truly model the phenomenon. An auxiliary load model is required.

A simplified model that is realistic to implement in OrcaFlex at the present stage is proposed based on the above fundamental assumptions. We are here inspired by equation (1), that is taken from Buchner (2002) [1].

3.1 Implementation in OrcaFlex

With reference to Figure 1, where a simplified pontoon geometry is seen from the side, the main steps of the model are as follows:

The pontoon is divided into N evenly spaced strips. At the center of each strip i, the incident (i.e. undisturbed) wave elevation $\zeta(y_i) \equiv \zeta_i$ is measured. From the undisturbed wave elevation, the total wave elevation including diffraction contributions is estimated as $\zeta_{i,tot} = \nu(y_i)\zeta_i$, where $\nu(y)$ is an amplification factor determined from a linear diffraction analysis. This will be addressed in a subsequent section. Then, the *upwell* at the strip is estimated as

$$\chi_i = \alpha(y_i)\zeta_{i,tot} - z_p(y_i), \tag{3}$$

Where $\alpha(y)$ is a wave asymmetry factor and $z_p(y_i)$ is the vertical motion of the pontoon's mean water line at strip i (i.e. $z_p(y_i) = 0$ in still water). This methodology is analogue with the one used to estimate air gap on semisubmersibles proposed in DNVGL-OTG-13 [4]. $z_p(y_i)$ can be calculated as

$$z_p(y_i) = \eta_3 - y_i\eta_4, \tag{4}$$

where η_3 is the heave motion and η_4 is the roll motion (in radians) of the pontoon. The vertical motion due to pitch is here neglected. Then, the freeboard exceedance is computed as

$$H(y_i) \equiv H_i = \begin{cases} \chi_i - s_0 & if \quad \chi_i > s_0 \\ 0 & otherwise \end{cases}. \tag{5}$$

The above calculation, that estimates if the freeboard is exceeded, and in case it is, the height of the water column on top of the strip, is performed for every strip at every time step of the simulation.

Having determined H_i, the resulting heave force at strip i is given as

$$F_z(y_i) \equiv F_{z,i} = \rho H_i \left(g + \ddot{z}_p(y_i)\right) A_i. \tag{6}$$

Here ρ is the water density, g is the acceleration of gravity, $\ddot{z}_p(y_i)$ is the vertical acceleration of the pontoon and A_i is the deck area of the pontoon at strip i. $\ddot{z}_p(y_i)$ can be estimated as

$$\ddot{z}_p(y_i) = \ddot{\eta}_3 - y_i\ddot{\eta}_4, \tag{7}$$

where $\ddot{\eta}_3$ and $\ddot{\eta}_4$ are the heave and roll accelerations, respectively.

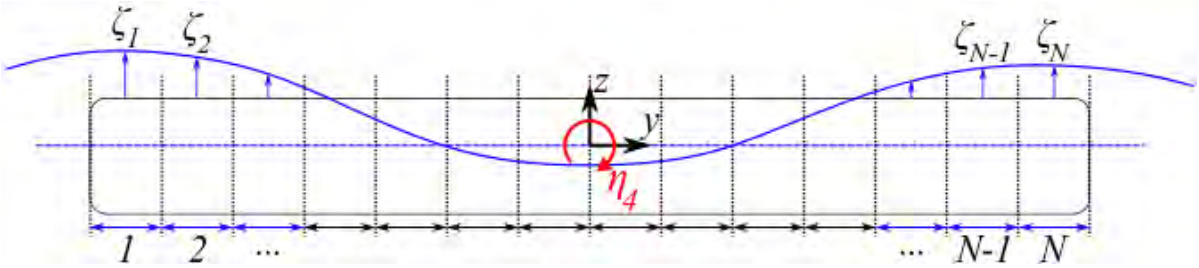

Figure 1 Principal sketch for simplified water-on-deck model seen from the side. In general the pontoon is moving, but is here shown in its mean position for simplicity. The pontoon is divided into N evenly spaced strips. ζ_i is the total wave elevation at the middle of strip i. Each strip has a deck area A_i, which is here assumed to be equal for all strips. s_0 is the freeboard in still water.

The global heave force and roll moment on a single pontoon is found from integration of the contributions from each strip, i.e.

$$\begin{aligned} F_z &= \sum_{i=1}^{N} F_z(y_i), \\ M_x &= \sum_{i=1}^{N} y_i F_z(y_i). \end{aligned} \tag{8}$$

A flow chart that illustrates the practical implementation of the model in the analysis is given in Figure 2.

1. At a given time instant t_n, OrcaFlex must provide the indicent wave elevation at each strip of each pontoon, and the motion and accelerations of each pontoon.
2. Using equations (3) - (8), heave forces and roll moments on each pontoon due to freeboard exceedance are computed.
3. The heave force $F_z(t_n)$ and roll moment $M_x(t_n)$ are applied to the OrcaFlex model as "Applied loads" in each column.
4. OrcaFlex integrates the solution forward in time to $t_n + \Delta t$.

5. Steps 1. – 4. above are repeated until the end of the simulation. In essence, the applied loads are included in the right-hand side of the equations of motion. Thus, $F_z(t_n)$ and $M_x(t_n)$ influences the floater's accelerations at t_n, and thus the new velocities and position estimated at $t_n + \Delta t$.

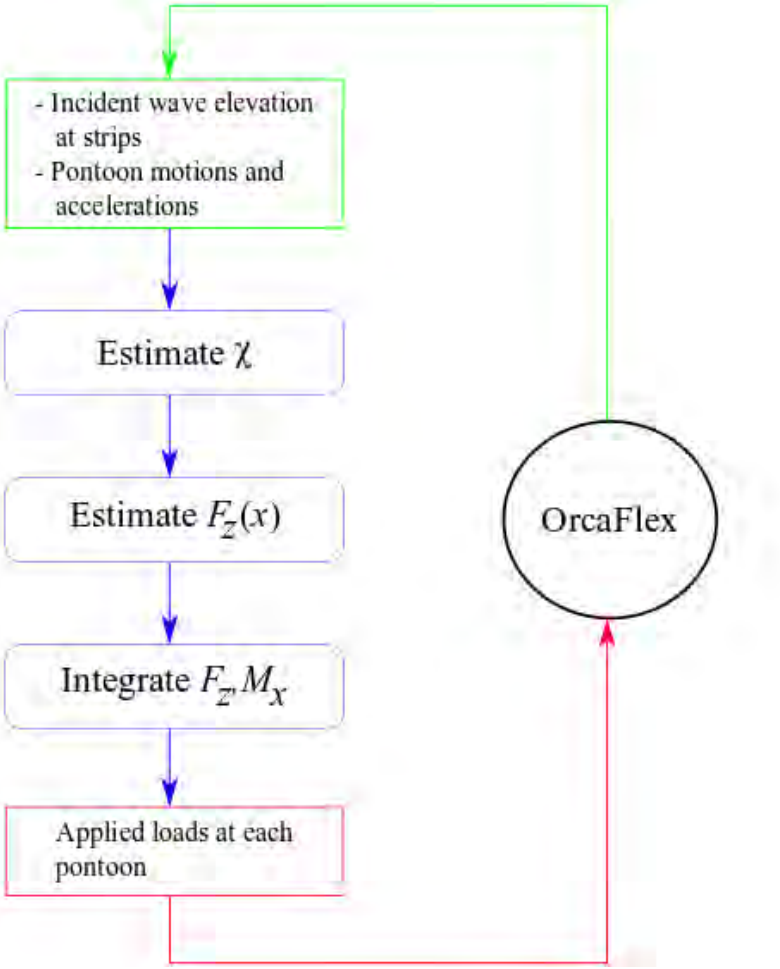

Figure 2 High-level flow chart for implementation of proposed model in OrcaFlex.

3.2 Assumptions and Simplifications

It is noted that surge and sway forces, and pitch and yaw moments, due to loss of freeboard are neglected in the present model. This is because they are assumed to be negligible compared to the resulting heave force and roll moment.

In connection with equation (6), it is assumed that H_i is uniform over each strip and equal to its value at the strip center.

3.3 The Model and its Relation with the Equations of Motion

Before we make any assumptions, the total fluid force on a body can be expressed as

$$\boldsymbol{F}(t) = \int_{S_B(t)} p(x,y,z,t)\boldsymbol{n}(x,y,z,t)dS, \tag{9}$$

where $S_B(t)$ is the body's instantaneous wetted surface, $p(x,y,z,t)$ is the total fluid pressure and $\boldsymbol{n}(x,y,z,t)$ is the instantaneous normal vector. A similar expression applies for the fluid moments. From Newton's 2nd law, we have that

$$\boldsymbol{M}\ddot{\boldsymbol{\eta}}(t) = \boldsymbol{F}(t) + \boldsymbol{F}_{add}(t), \tag{10}$$

Where $\boldsymbol{F}_{add}(t)$ are additional forces due to e.g. mooring lines or viscous damping. Note here that the force vector $\boldsymbol{F}(t)$ contains both hydrostatic and dynamic loads. So far we have made no assumptions (other than implicitly stating that potential-flow theory applies). In order to solve the equations of motion in a practical manner, it is common to split the right-hand side of (10) into

contributions that are proportional to the body's velocity and position. This is also done in OrcaFlex. If we now assume a pure uncoupled heave motion without any mooring system or additional damping, this can be written

$$(M + A_{33})\ddot{\eta}_3 + B_{33}\dot{\eta}_3 + C_{33}\eta_3 = F_z(t), \tag{11}$$

where the right-hand side is given by (8). In going from the general expression in (10) to (11), we have introduced assumptions about linearity that are as follows:

- The fluid force in phase with the body's acceleration is expressed as an added-mass force $-A_{33}\ddot{\eta}_3$.
- The fluid force in phase with the body's velocity is expressed as a damping force $-B_{33}\dot{\eta}_3$.
- The fluid force in phase with the body's motion is expressed as a restoring force $-C_{33}\eta_3$.
- The fluid force due to change in pressure (due to the relative wave elevation) is accounted for by the force $F_z(t)$.

This point is made in order to emphasise that when we write an equation of motion as in (11), we have to be aware of the underlying assumptions. Since OrcaFlex writes the equations of motion in this form, this says something about the hydrostatic force: C_{33} represents the change in hydrostatic force as a function of a heave displacement. This is a linear term, i.e. if η_3 is doubled, so is $C_{33}\eta_3$. If we like to, we can introduce non-linearity in C_{33}, e.g. $C_{33} = C_{33}(\eta_3)$ so that the restoring coefficient is a function of the heave motion. However, the restoring force is still strictly a function of the heave motion relative to the still-water position. The way that the equation of motion is formulated in (11), the wave elevation can never lead to a modification of C_{33}. To illustrate why, consider some simplified examples:

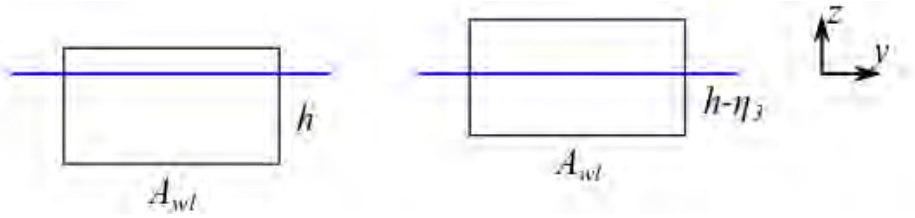

Figure 3 A simple box in still water. Left: No heave motion, right: Heave motion η_3.

Figure 4 A simple box in still water with uniform layer of water with height H on deck. Left: No heave motion, right: Heave motion η_3.

First we consider Figure 3. Let the left configuration be denoted (1) and the right (2). The hydrostatic force in z direction for the two cases are

$$F_z^{(1)} = -\rho g(-h)A_{wl}$$
$$F_z^{(2)} = -\rho g\big(-(h-\eta_3)\big)A_{wl}.$$

The difference between the two is

$$\Delta F_z = F_z^{(2)} - F_z^{(1)} = -\rho g \eta_3 A_{wl}.$$

By setting $\Delta\eta_3 = \eta_3$, we get

$$\frac{\Delta F_z}{\Delta\eta_3} = -\rho g A_{wl} = C_{33}.$$

This shows that C_{33} represents the change in the hydrostatic force as a function of the heave motion.

Then we consider the case in Figure 4, where a constant volume of water on deck is added to the scenario in Figure 3. Since we are in hydrostatic condition, the weight of this water is

$$F_z = -\rho g H A_{wl}.$$

We then again write out the expression for the two configurations (1) and (2) and take the difference between them:

$$F_z^{(1)} = -\rho g(-h)A_{wl} - \rho g H A_{wl}$$
$$F_z^{(2)} = -\rho g\big(-(h-\eta_3)\big)A_{wl} - \rho g H A_{wl}.$$
$$\Delta F_z = F_z^{(2)} - F_z^{(1)} = -\rho g \eta_3 A_{wl}.$$

From this, we get

$$\frac{\Delta F_z}{\Delta\eta_3} = -\rho g A_{wl} = C_{33}.$$

Hence, C_{33} is not affected by the water on deck in the equation of motion (11). ***That is not to say that the water on deck does not have an effect on the system that may affect its stability, but it is not to be taken into account in the restoring terms in the equations of motion.***

3.4 Introducing Non-Linearity into Restoring Coefficients

As follows from the discussion in the previous section, the only time it is relevant to modify C_{33} (and the other restoring terms C_{ij}), is if the bridge's motion is so that parts of it come below the still-water level. Such scenario is illustrated in Figure 5.

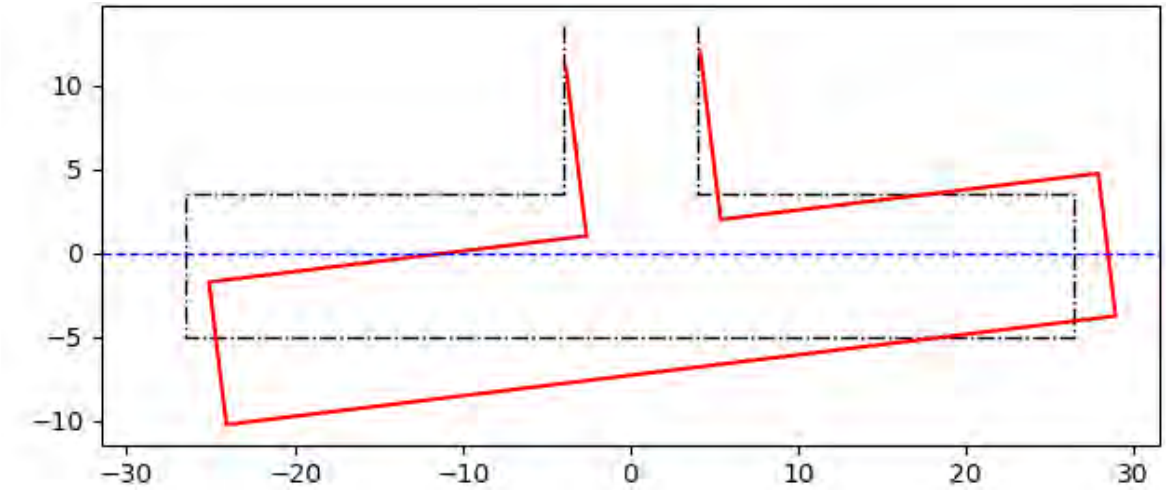

Figure 5 Scenario where pontoon comes partially below still-water level.

To manage with this scenario, we can introduce modified restoring coefficients $C_{ij}(\boldsymbol{\eta}) = C_{ij} + \Delta C_{ij}(\boldsymbol{\eta})$, where C_{ij} is the original restoring coefficient in degree of freedom i due to motion in degree of freedom j. The equation of motion in (11) for motion in degree of freedom i would then read

$$\sum_{j=1}^{6}\big(M_{ij} + A_{ij}\big)\ddot{\eta}_j + B_{ij}\dot{\eta}_j + C_{ij}\eta_j = F_i(t) - \sum_{j=1}^{6}\Delta C_{ij}(\boldsymbol{\eta})\eta_j, \qquad (12)$$

Where $F_i(t)$ is the water-on-deck loading in degree of freedom i. The terms associated with $\Delta C_{ij}(\boldsymbol{\eta})$ are here moved to the right-hand side of the equation, because we in practice would like to include this load as an applied load in the analysis. As a first step, we will include a check in the analysis to detect along each strip in Figure 1 if the vertical position of the deck becomes lower than the still waterline. In the ULS condition, a preliminary assessment has shown that this is unlikely to occur. However, in the case that the deck level should move below the still water level, we will consider carefully how to express $\Delta C_{ij}(\boldsymbol{\eta})$. If, on the other hand, this never occurs, the restoring terms need never be modified.

For further elaboration, we may consider a simplified pontoon in still water in Figure 6, that is either surface-piercing (1) or submerged (2). We assume that the area of the pontoon projected onto the xy plane is S_0, and that the column has area S_C.

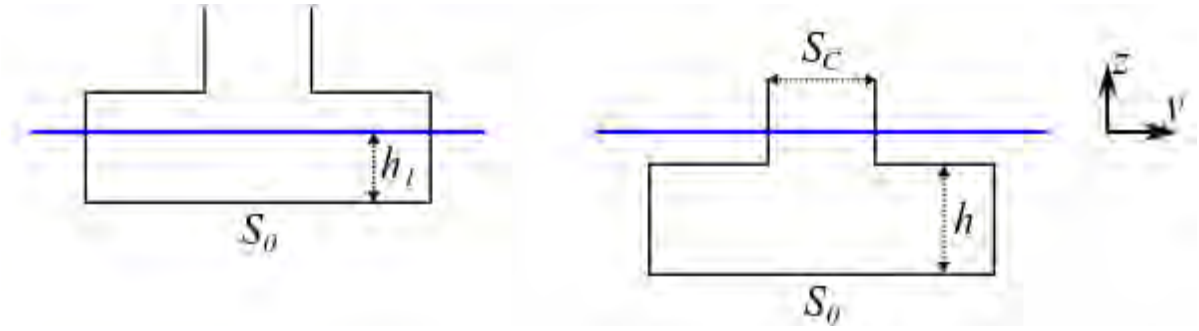

(1) (2)

Figure 6 Pontoon in surface-piercing and submerged positions.

In (1), we have that

$$F_z^{(1)} = \rho g h_1 S_0.$$

Where h_1 is the draught. In (2), we have that

$$F_z^{(2)} = \rho g (h + h_t) S_0 - \rho g h_t (S_0 - S_c).$$

where h is the pontoon height and h_t is the distance from the still-water level to the top of the pontoon. Clearly,

$$\Delta F_z = F_z^{(2)} - F_z^{(1)} \neq -\rho g \eta_3 S_0.$$

In the context of the equation of motion (11), one could be tempted to account for such difference by estimating and equivalent water-plane restoring coefficient. However, for an irregular type of response, this is not possible to do in a rational manner. Hence, such difference should rather be accounted for by $\Delta C_{ij}(\boldsymbol{\eta})$ terms such as outlined in (12).

3.5 Wave Amplification due to Diffraction and Non-Linear Effects

The amplification of the incident wave due to linear diffraction effects around the cylinder, that here are approximated by the factor $v(y_i)$, are determined from a linear diffraction analysis in Wadam. In order to be practical, a single value for the entire pontoon length (i.e. independent of strip) is chosen. This is an assumption that includes considerable conservatism, as the diffraction effect strongly varies with location, wave direction and wave period. In addition, it is assumed that the contribution from the radiation potential is limited, so that the pontoon is fixed in the hydrodynamic analysis. This assumption may be checked by doing diffraction analysis with a freely floating body. However, it is then of key importance that we represent correctly the pontoon stiffness in different degrees of freedom. This stiffness is not only due to hydrostatic restoring, but also because the pontoon belongs to a larger coupled dynamic system.

Result plots showing the wave amplification factors for some relevant wave periods and wave directions are given in Figure 7 - Figure 10. The results are summarized in a pragmatic manner below:

Table 1 Wave amplification near pontoon bow region.

Wave period	***Wave direction relative to pontoon axis***		
	0°	10°	30°
4 s	1.8	1.8	1.8
5 s	1.6	1.6	1.6
6.25 s	1.4	1.4	1.4
8 s	1.2	1.2	1.2

Table 2 Wave amplification near pontoon side.

Wave period	***Wave direction relative to pontoon axis***		
	0°	10°	30°
4 s	1.2	1.3	2.0
5 s	1.1	1.3	1.8
6.25 s	1.1	1.2	1.5
8 s	1.0	1.1	1.2

Note that the effect of wave-current interaction on upwell here is disregarded. This effect may be checked by e.g. a Wasim analysis.

In the 100 year condition, the sea state expected to be governing has $H_s = 2.1\ m, T_p = 5.2\ s$ [5]. In a conservative way, we then set $\nu(y_i) \equiv \nu = 1.8$. That means that the diffracted wave elevation is taken as 1.8 times the undisturbed wave.

The wave asymmetry factor α in equation (3) takes into consideration non-linear effects in the incident wave itself and non-linear effects due to wave-body interaction. For an offshore structure, α values in the range 1.2 – 1.3 are typical [6]. This is related to strongly non-linear wave amplification effects. Here, where the motions are small and with moderate waves, we assume that a wave asymmetry factor $\alpha = 1.2$ can be used throughout (i.e. α is equal for all strips).

Using the proposed values for $\nu(y_i)$ and α in the present section, we have all the tools required to implement the model in (3) - (8) in OrcaFlex. As mentioned, this represents an approximate model that is built taking into account the relevant physical effects. In the next chapter, we briefly mention a strategy that can be relevant to implement at a later stage for a more accurate modelling.

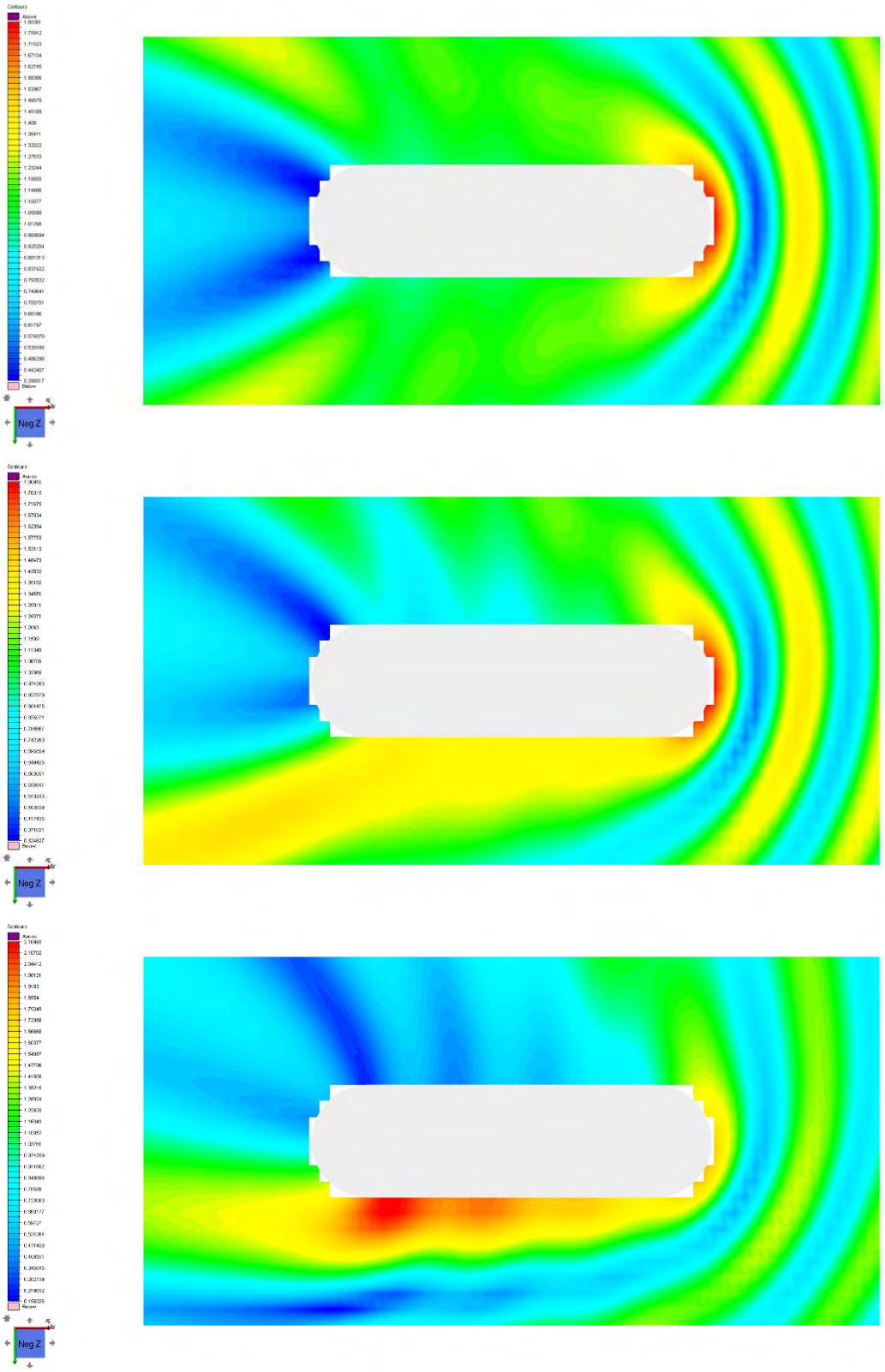

Figure 7 Wave elevation RAO around fixed pontoon for waves aligned with, 10° and 30° relative to longitudinal pontoon axis for regular waves with period T = 4.00 s.

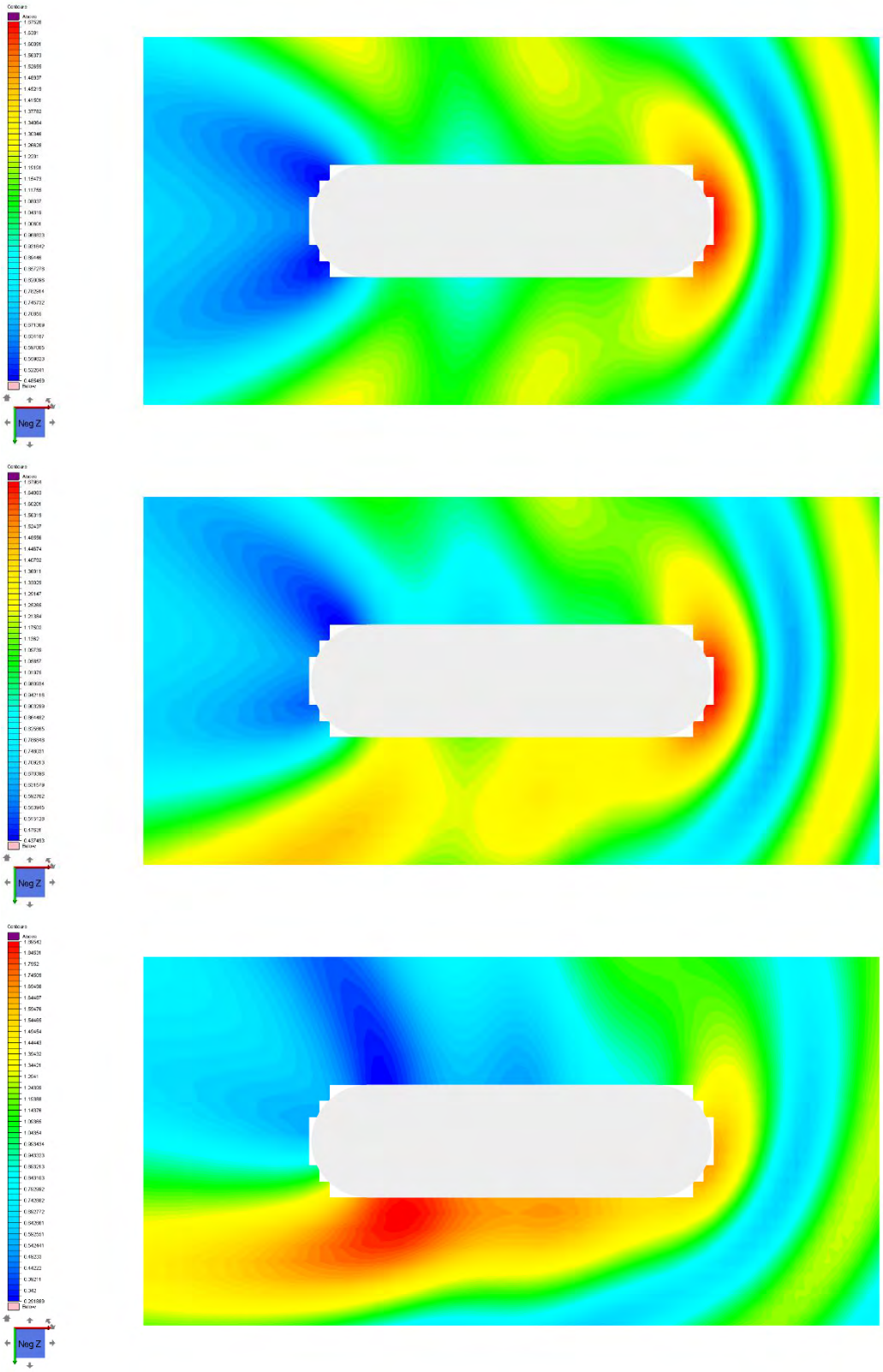

Figure 8 Wave elevation RAO around fixed pontoon for waves aligned with, 10° and 30° relative to longitudinal pontoon axis for regular waves with period T = 5.00 s.

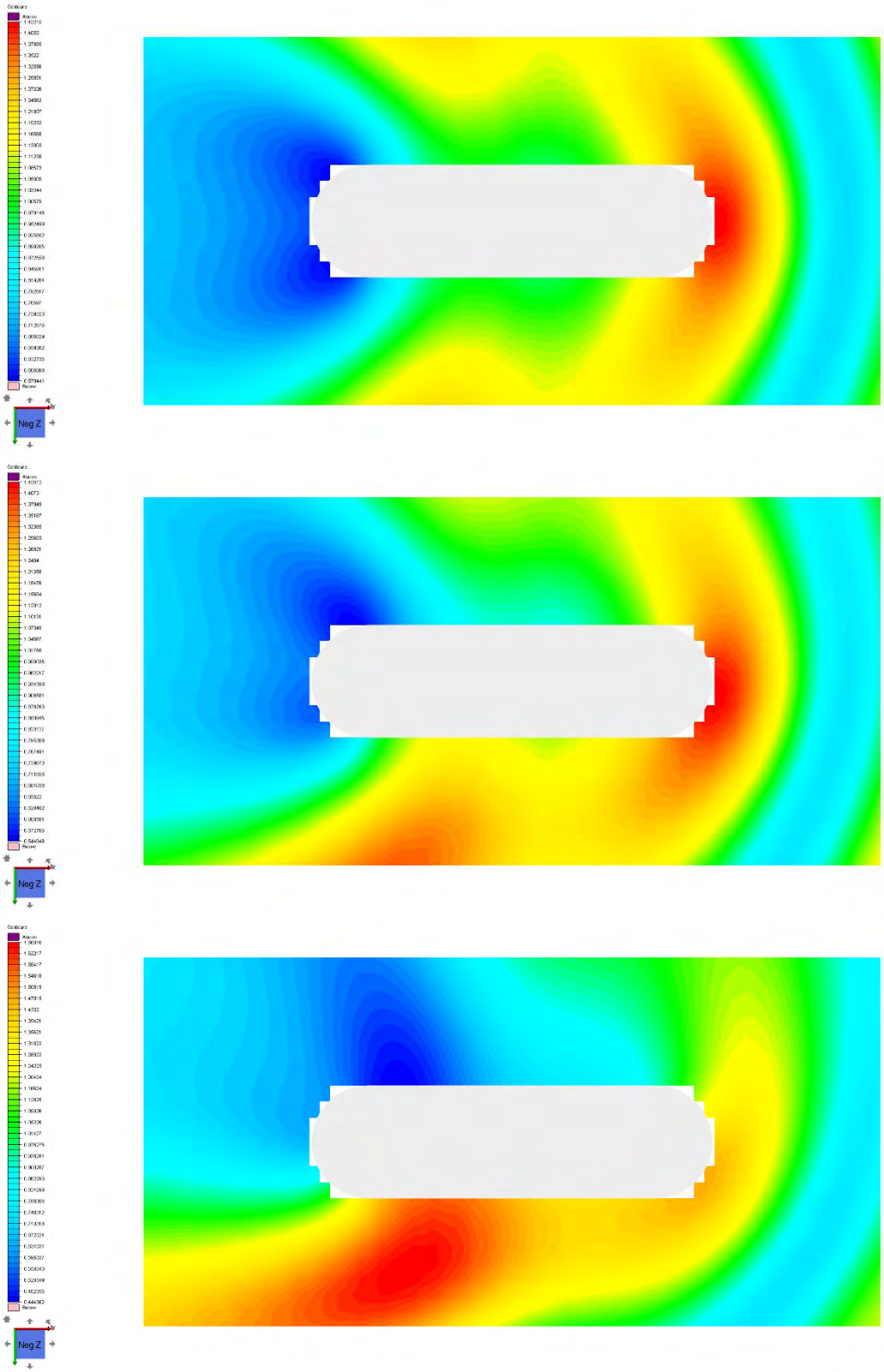

Figure 9 Wave elevation RAO around fixed pontoon for waves aligned with, 10° and 30° relative to longitudinal pontoon axis for regular waves with period T = 6.25 s.

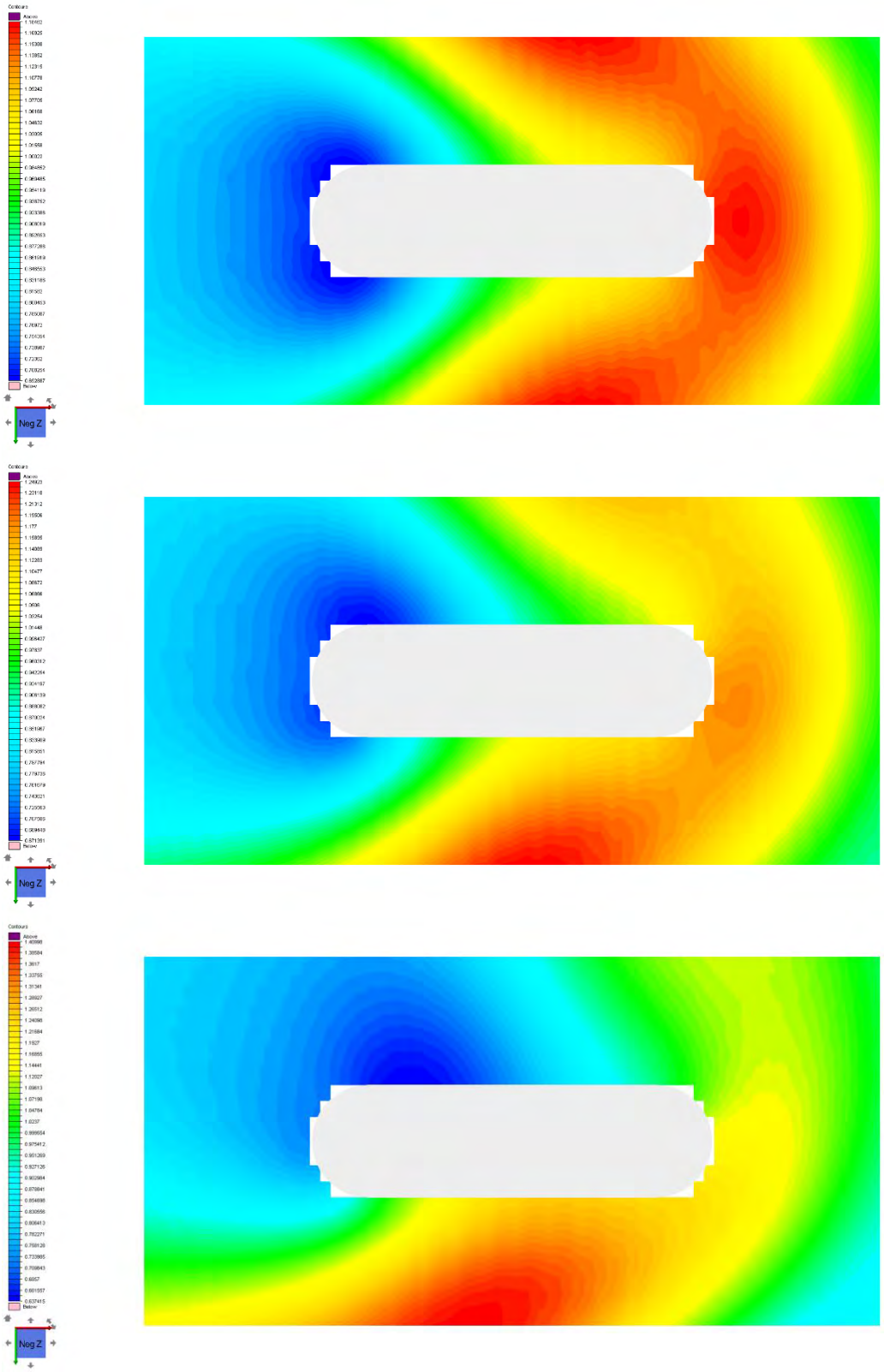

Figure 10 Wave elevation RAO around fixed pontoon for waves aligned with, 10° and 30° relative to longitudinal pontoon axis for regular waves with period T = 8.00 s.

4 Proposed Enhanced Model for In-Depth Studies at a Later Stage

In order for a more in-depth assessment of the effect of freeboard loss at a later stage of the project, two possibilities are proposed:

1. Perform a CFD analysis for some selected or generic events where freeboard is lost in order to better understand the physics of the particular problem, and to investigate the magnitude of resulting forces and moments on the pontoon. Here also the horizontal wave impact loads on the column can be quantified.
2. Implement a shallow-water model, such as done by Greco & Lugni (2012) [2]. This is anticipated to be a rather time consuming task, and before doing so, one should assess the importance of the water-on-deck events on the global behaviour of the bridge. The simplified model proposed for the present phase is instructive in this respect.
3. Preferrably in combination with either of the two above, dedicated model tests should be performed where the setup is defined in such a way to clearly investigate the freeboard-exceedance events. Such targeted model tests require firm planning.

5 References

[1] B. Buchner, “Green Water on Ship-type Offshore Structures,” 2002.

[2] M. Greco and C. Lugni, “3-D seakeeping analysis with water on deck and slamming. Part 1: Numerical solver,” *Journal of Fluids and Structures,* no. 33, pp. 127-147, 2012.

[3] L. Wan, M. Greco, C. Lugni, Z. Gao and T. Moan, “A combined winf and wave energy-converter concept in survival mode: Numerical and experimental study in regular waves with a focus on water entry and exit,” *Applied Ocean Research,* no. 63, pp. 200-216, 2017.

[4] DNV GL, “Offshore Technical Guidance DNVGL-OTG-13 Prediction of air gap for column, Edition March 2017,” 2017.

[5] Statens vegvesen, “SBJ-01-C4-SVV-01-BA-001 MetOcean Design basis, rev. 1,” 2018.

[6] DNV GL, “DNVGL-RP-C205, Environmental conditions and environmental loads,” 2017.

[7] Multiconsult, “BJØRNAFJORDEN, STRAIGHT FLOATING BRIDGE PHASE 3, Analysis and design (Base Case), BJ-31-C3-MUL-22-RE-100,” 2017.

[8] Statens vegvesen, “Design Basis Bjørnafjorden floating bridges rev. 0,” 2018.

Concept development, floating bridge
E39 Bjørnafjorden

Appendix H – Enclosure 2

CMA-19-008-MCO-RT-001

Pontoon CFD

CoreMarine
SMART OCEAN SOLUTIONS

DOCUMENT NO: CMA-19-008-MCO-RT-001 PONTOON CFD

B4		CLO	OJO	BFI	Initials
		22/05/2019	28/05/2019		Date
		B4	B1		Signature
Revision Number	**Description**	**Prepared**	**Checked**	**Approved**	**Approved**

Revision History

Revision Number	Date	Section(s)	Page(s)	Brief Description of Change	Author of Change
B2	13/06/2019			Comments from clients.	CLO
B3	23/06/2019	Section 6		Additional results section (section 6) Included	CLO
B4	12/08/2019	Section 7		Additional Fluid domain size 2D Check	CLO

TABLE OF CONTENTS

1 INTRODUCTION

This document describes the CFD numerical model generated to model the steady drag and oscillatory fluid flow around a pontoon structure to support a floating bridge designed by AMC (Aas-Jakobsen, Multiconsult and COWI).

The main objective of the study is to obtain towing resistance for marine operation and oscillatory drag and added mass coefficient to be used in time domain simulation.

Two main condition are analysed:

1. Marine Operation: Structure supporting steady current (3knots) at different heading angles.
2. KC condition: Structure supporting oscillatory fluid flow at different KC numbers and no steady current and 0deg heading

For all case the draft is fixed at 5m

No free surface on the CFD model has been used for the main results obtained in this study, the free surface is modelled as a Free sleep wall.

2 EXECUTIVE SUMMARY

The main result of Steady current shows an approx. value of Cd=0.4 for 0 deg heading.

		HULL1	HULL2	HULL3	HULL4	HULL5	HULL_bot	Total Force	Total Force
		kN	kN	kN	kN	kN	kN	kN	Tonne
0deg 3kts	Fx	-7.3	-7.4	-7.7	-8.1	-6.0	-1.0	-37.4	-3.8
	Fy	0.0	0.0	0.0	0.0	0.1	0.0	0.2	0.0
15 deg 3kts	Fx	-9.4	-9.6	-9.9	-9.9	-6.0	-2.0	-46.7	-4.8
	Fy	9.7	9.7	9.6	8.9	3.8	-0.3	41.4	4.2
30 deg 3kts	Fx	-22.7	-22.4	-21.8	-20.3	-10.1	-2.3	-99.6	-10.1
	Fy	25.7	26.0	25.6	23.0	10.9	-1.6	109.6	11.2
90 deg 3kts	Fx	-72.8	-71.2	-68.8	-63.4	-41.7	0.6	-317.3	-32.3
	Fy	0.0	0.0	0.0	0.0	0.0	0.6	0.6	0.1

Table 1 : Sectional Loads for steady current

The sectional values for steady current provide a relatively constant value of CD along the different sections. The normalizing area used for Cd is transverse dimension (14.9m) multiplied by the section height.

Cd	HULL1	HULL2	HULL3	HULL4	HULL5
0deg 3kts	0.40	0.41	0.42	0.44	0.33

Table 2 : Drag Coef for =deg Steady Current

The Period selected for all KC study is 15s. The oscillatory velocity amplitude is varied according to selected KC values provided by MULTICONSULT

For the KC study it is observed a very consistent value of Added mass in the range of 530 to 590t

The oscillatory damping is more dependent on KC number compared to Added mass coef.

	KC = 0.5	KC = 1	KC = 2	KC = 3	KC = 4
Phase (deg)	-1.93	-2.02	-2.54	-3.10	-3.82
Force total Amplitude 1s Order (N)	9.09E+05	1.80E+06	3.64E+06	5.47E+06	7323790.45
Force inertia amplitude (N)	9.08E+05	1.80E+06	3.64E+06	5.46E+06	7307481.67
Force viscous amplitude (N)	3.06E+04	6.35E+04	1.62E+05	2.96E+05	488485.68
Second Order Force Amplitude RMS (N)	5.88E+03	1.12E+04	1.98E+04	3.19E+04	45882.73
					0.00
Pontoon total Mass (t) (displacement · water density)	3803.0	3803.0	3803.0	3803.0	3803.04
Added Mass (t)	564.4	531.2	569.9	575.7	589
Damping (kN/(m/s))	61.6	64.0	81.4	99.4	122.98

Table 3 : KC study Main Results

3 CONCEPT DESCRIPTION

Client provide the following geometry on mail 02/05/2019

Main Draft is 5m. The total displaced mass is 3803t

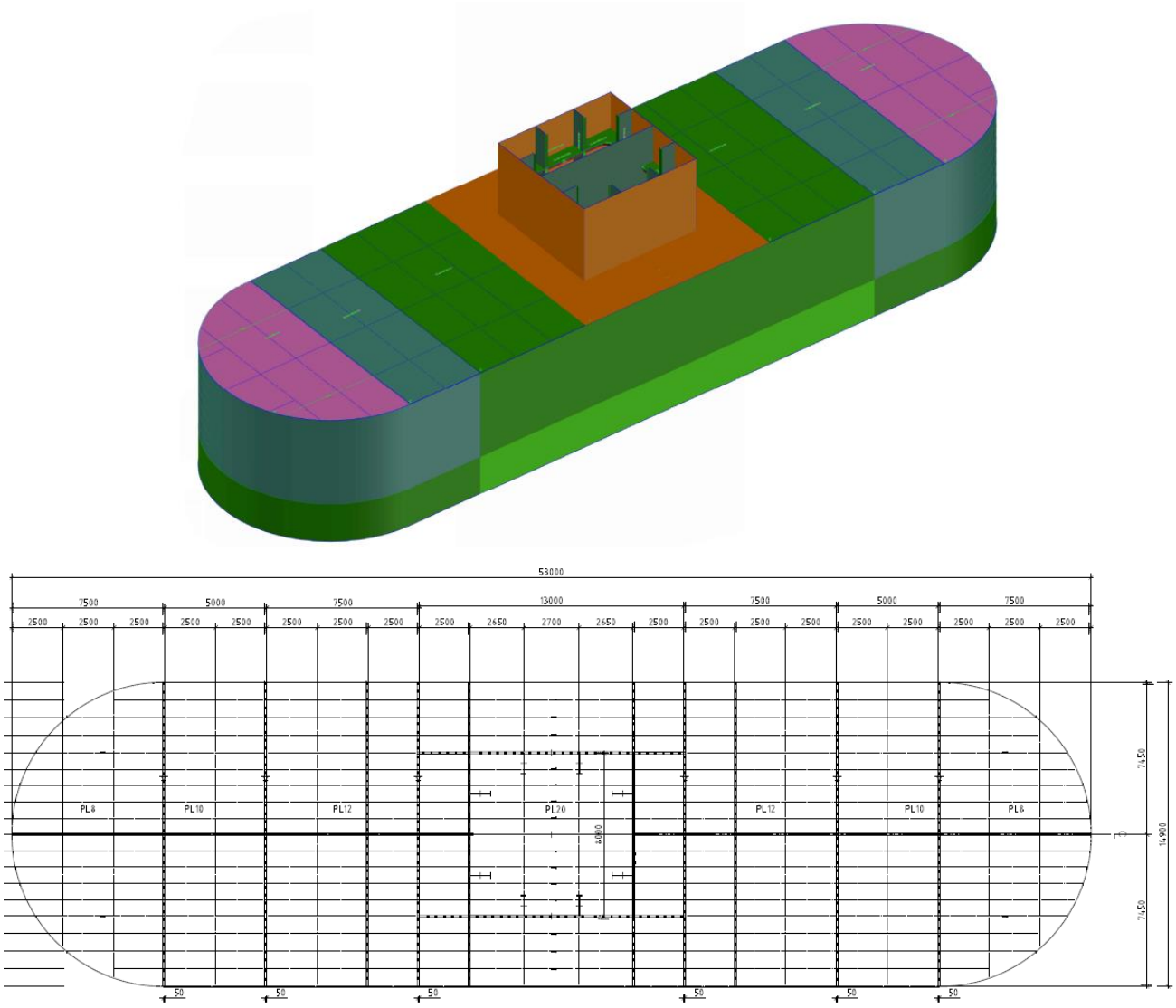

Figure 1 : Geometry Provided

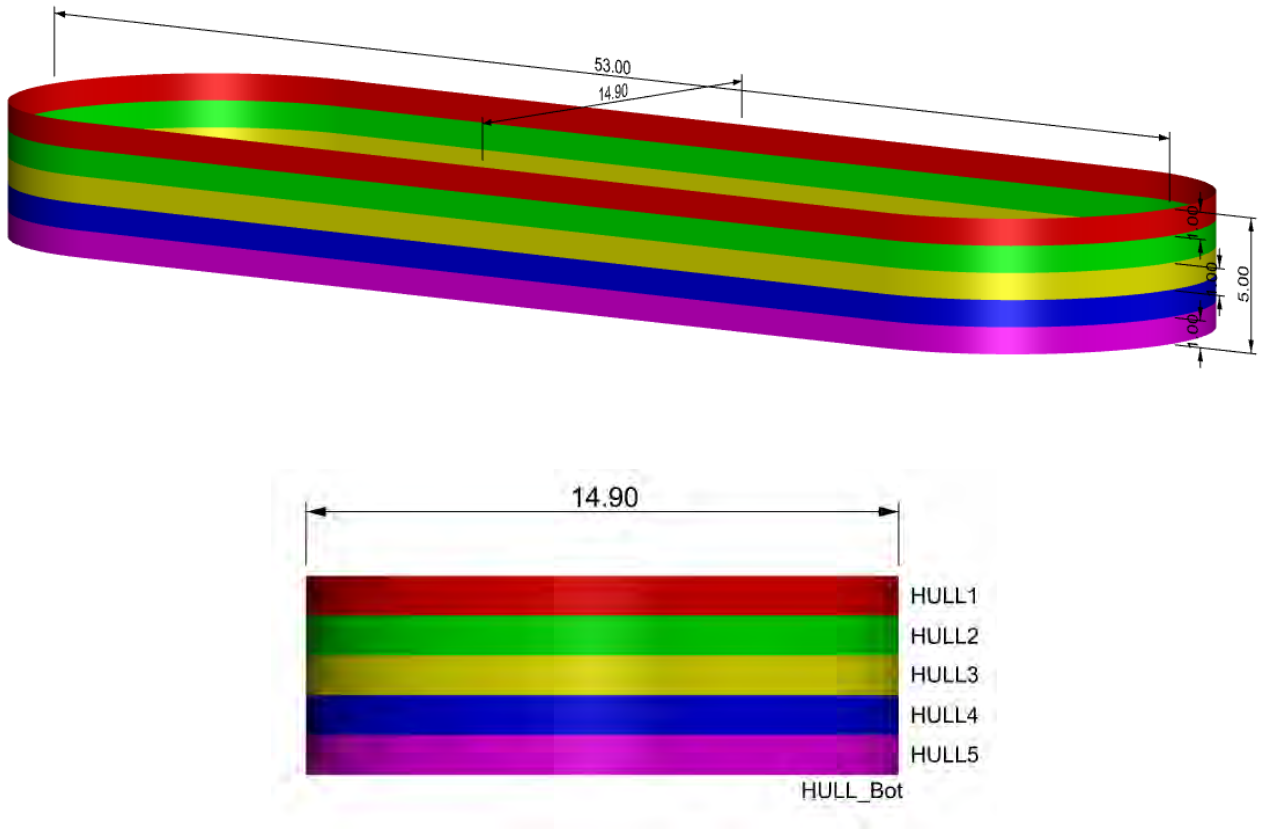

Figure 2 : Geometry modelled

The geometry is 3d modelled and divided in 5 vertical section and the bottom plate. Each section will be meshed independently and drag result can be integrated in each section in the complete 3D model, allowing a determination of the drag coef and added mass for 1m thickness sections. This strategy does not affect the global drag results, only affect the postprocessing allowing a differentiated postprocessing of the different sections.

The Structure is meshed with structured mesh and inflation layer for a more refined and controllable mesh size on the near wall zone.

The fluid domain for 3D full CFD is 250x250m and 50m water deep. This is considered enough to prevent any blockage effect as recommended by ITTC – Recommended Procedures and Guidelines 7.5 – 03 – 02 – 03 where a 1-2 Lpp is recommended for any boundary condition to be from vessel.

1.1 REFERENCE FRAMES AND CONVENTIONS.

- Pontoon centre is located at origin, hull flotation level is position is Z=0. Bottom plate of pontoon is located at z=-5m. (Means: Origin is in the still water line and pontoon horizontal centre. The draft is 5m.)
- X is in the pontoon longitudinal direction and Z vertical and positive upwards. Steady current is applied in negative X direction giving negative drag forces.

4 MODEL DESCRIPTION

The numerical model software used in this work has been OpenFOAM (Open Field Operation And Manipulation), which includes solver and specific boundary conditions for wave generation and absorption. This version of the model adapted for wave and structure inter-action was first introduced by (Pablo Higuera, 2013) and is known as IHFOAM. The numerical model solves the three-dimensional Reynolds Averaged Navier–Stokes (RANS) equations for two incompressible phases using a finite volume discretization and the volume of fluid (VOF) method. In VOF, each phase (i) is described by the fraction(αi) occupied by the volume of fluid of the material in each cell. The new solver supports several turbulence models (e.g.,k-ε,k-ω SST and LES). The aforementioned RANS equations, which include continuity and momentum conservation equations link the pressure and velocity

IHFOAM is a three-dimensional numerical two-phase flow solver specially designed to simulate coastal, offshore and hydraulic engineering processes. Its core is based on OpenFOAM®, a very advanced Multiphysics model, widely used in the industry. (A. Iturrioz, 2015)

5 2D CASE PRELIMINARY TEST

A 2D geometry model has been generated to performed initial time step and mesh sensitivity analysis.

Three 2D structured hexahedral mesh has been generated with the following characteristics

- 2D mesh A (Figure 3): 1 layer thickness: 20000 elements 20 inflation layers for wall elements (initial wall layer thickness 0.1mm.
- 2D mesh B (Figure 4): 1 layer thickness: 100000 elements 40 inflation layers for wall elements. (initial wall layer thickness 0.1mm.
- 2D mesh C (Figure 5): 1 layer thickness: 800000 elements 80 inflation layers for wall elements. (initial wall layer thickness 0.1mm.

The CFD model has the following characteristics

- Fix model (no sink and trim).
- Multi-Phase VOF Solver (solving only water phase, no free surface)
- Steady State Calculation for Steady current and Transient for KC test.
- Specified velocity at inlet corresponding to current speed.
- Lateral top and bottom walls, Fee slipping walls with no roughness.
- Turbulence model: SST.
- Hull wall, No slip wall, with different roughness (0, 1 and 5mm)
- Water Density 1025 kg/m^3
- Kinematic Viscosity 1.04E-06 m2/s

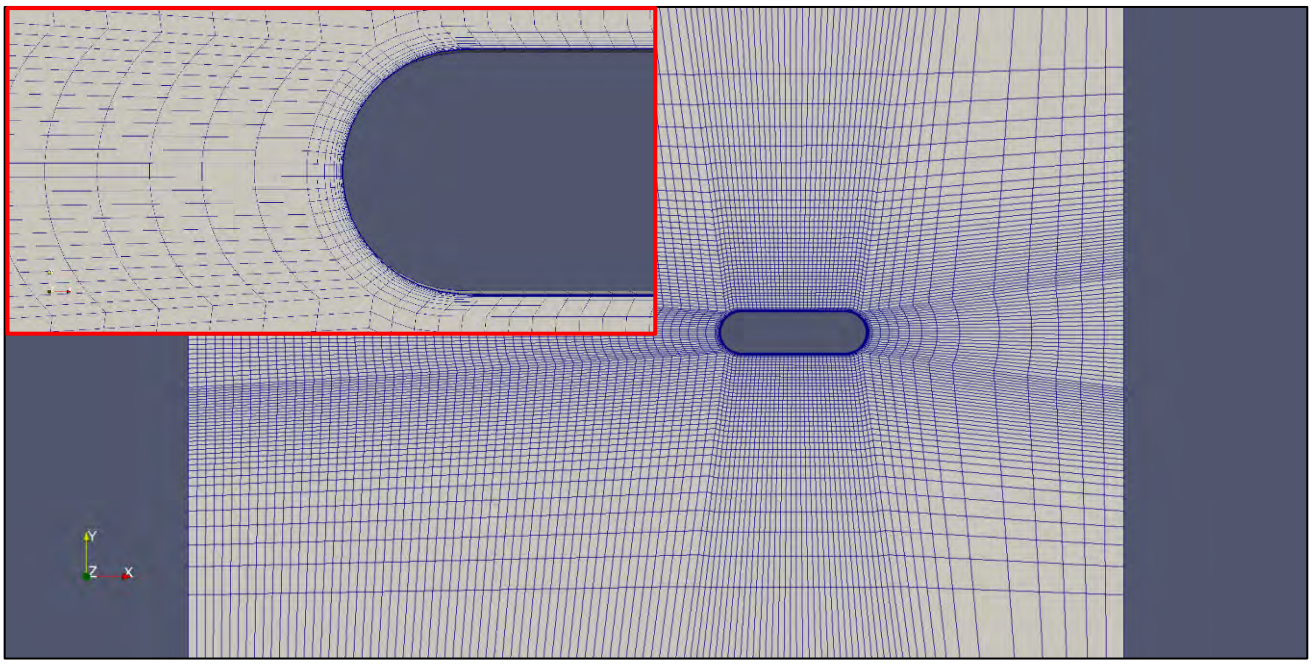

Figure 3 : Mesh A (2D).

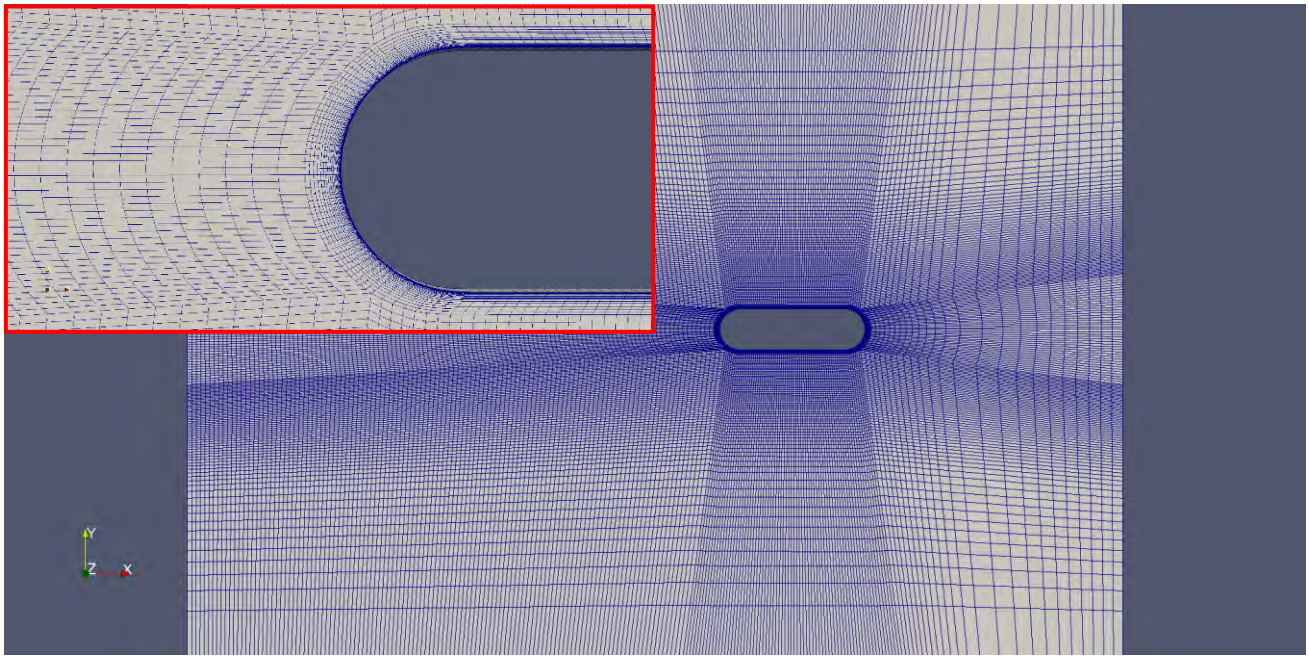

Figure 4 : Mesh B (2D).

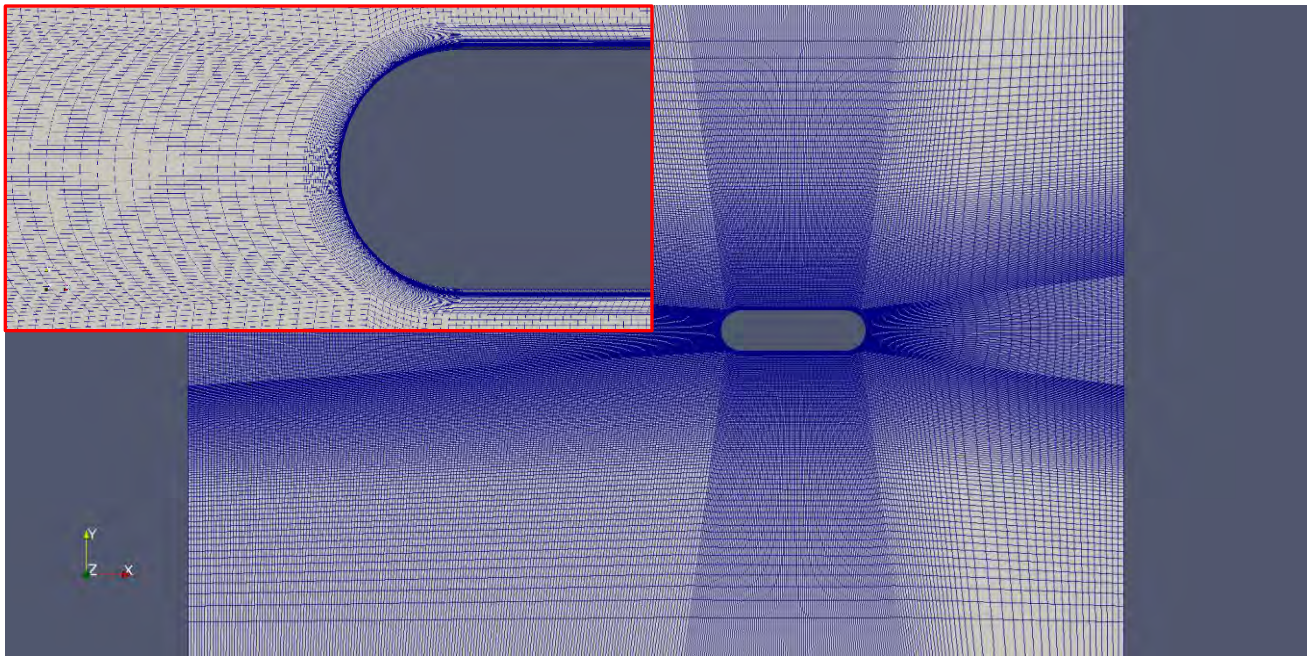

Figure 5 : Mesh C (2D).

5.1 TIME STEP CONVERGENCE.

Different time steps are tested and convergence to same value is detected. Convergence is tested for Mesh B where the Courant number is approx. 0.4 for 0.1s; Approx. 1.0 for 0.25s and Approx. 2.0 for 0.5s.

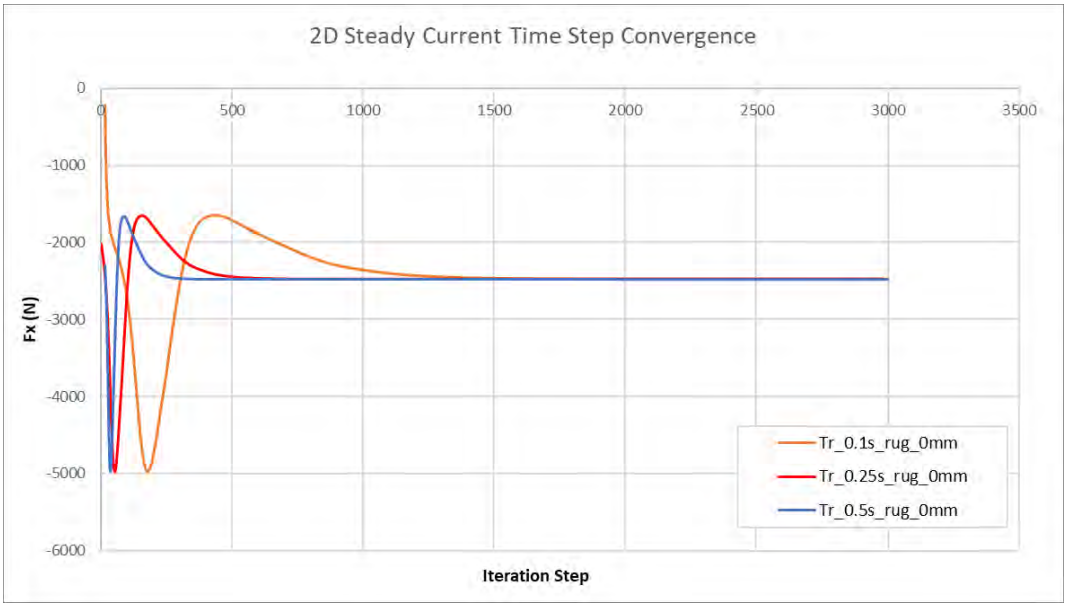

Figure 6 : Time step convergence Study.

Time step of 0.25 is selected for further analysis been the one corresponding to Courant Nº=1.

5.2 MESH SIZE CONVERGENCE STUDY.

The 3 generated mesh are tested at 0.25s Time Step

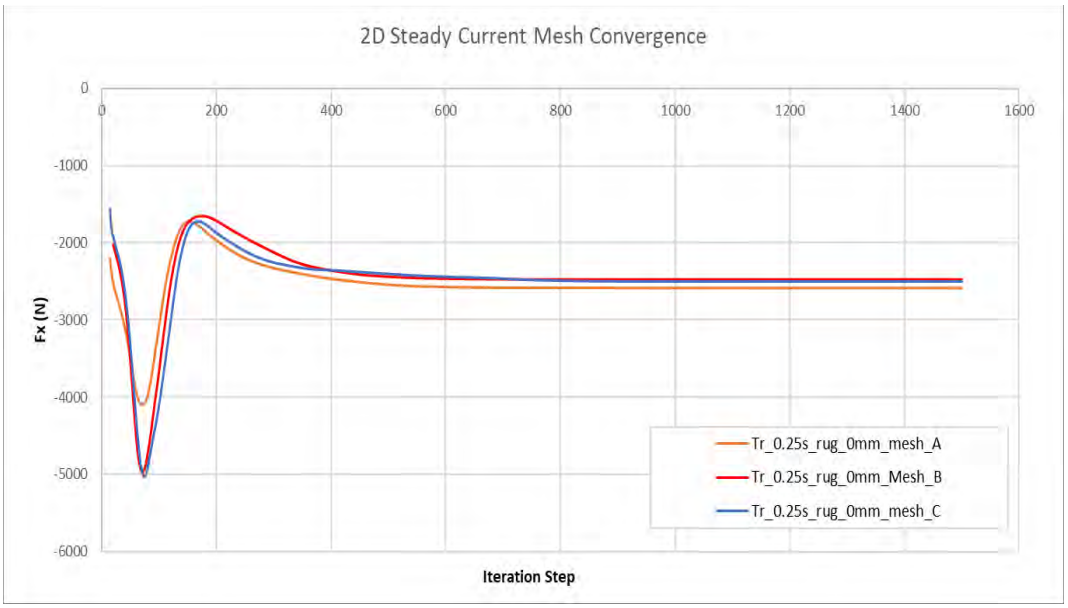

Figure 7 : Mesh convergence Study.

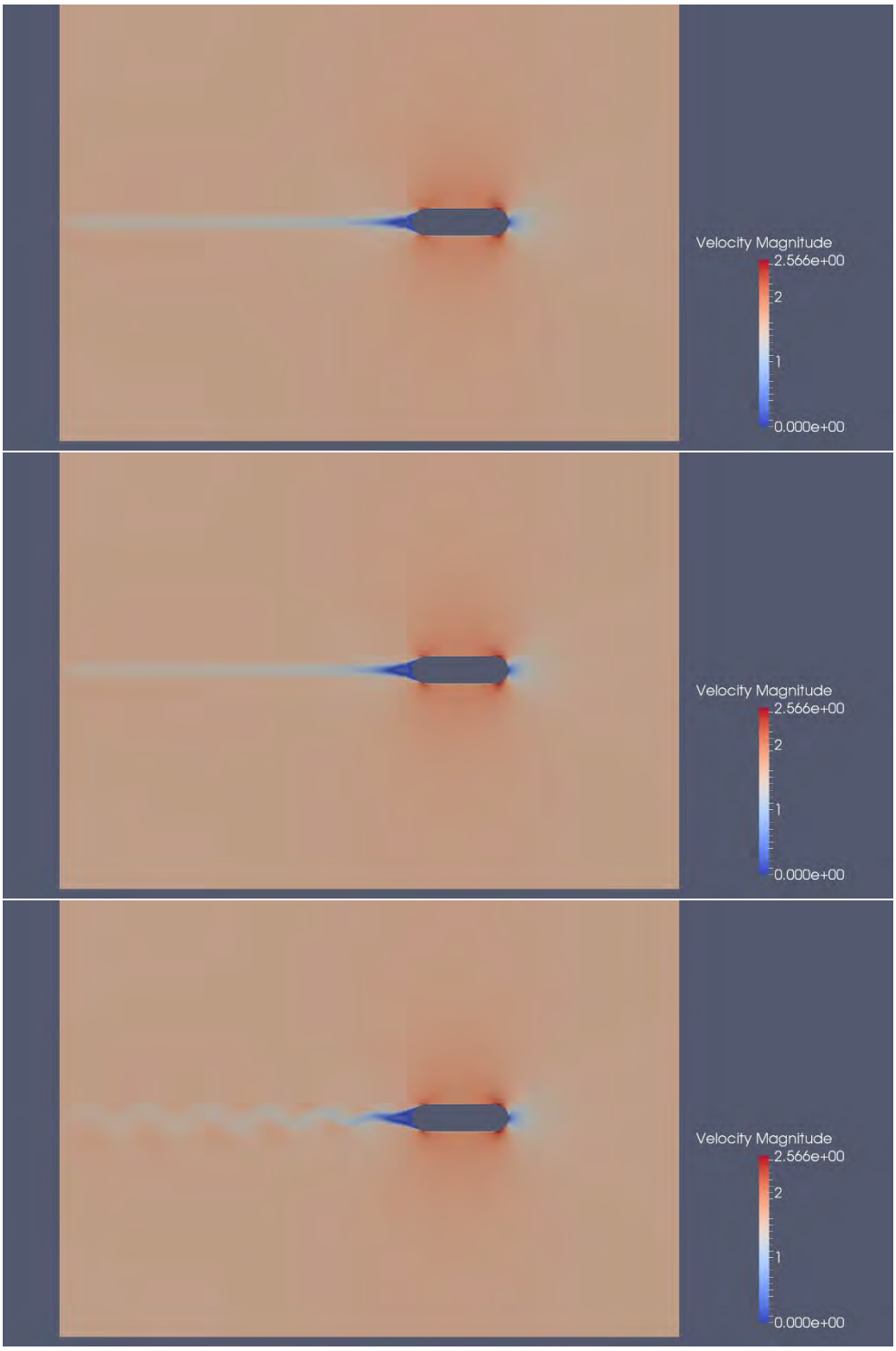

Figure 8 : Mesh convergence Mesh A, B and C (steady current 2D)

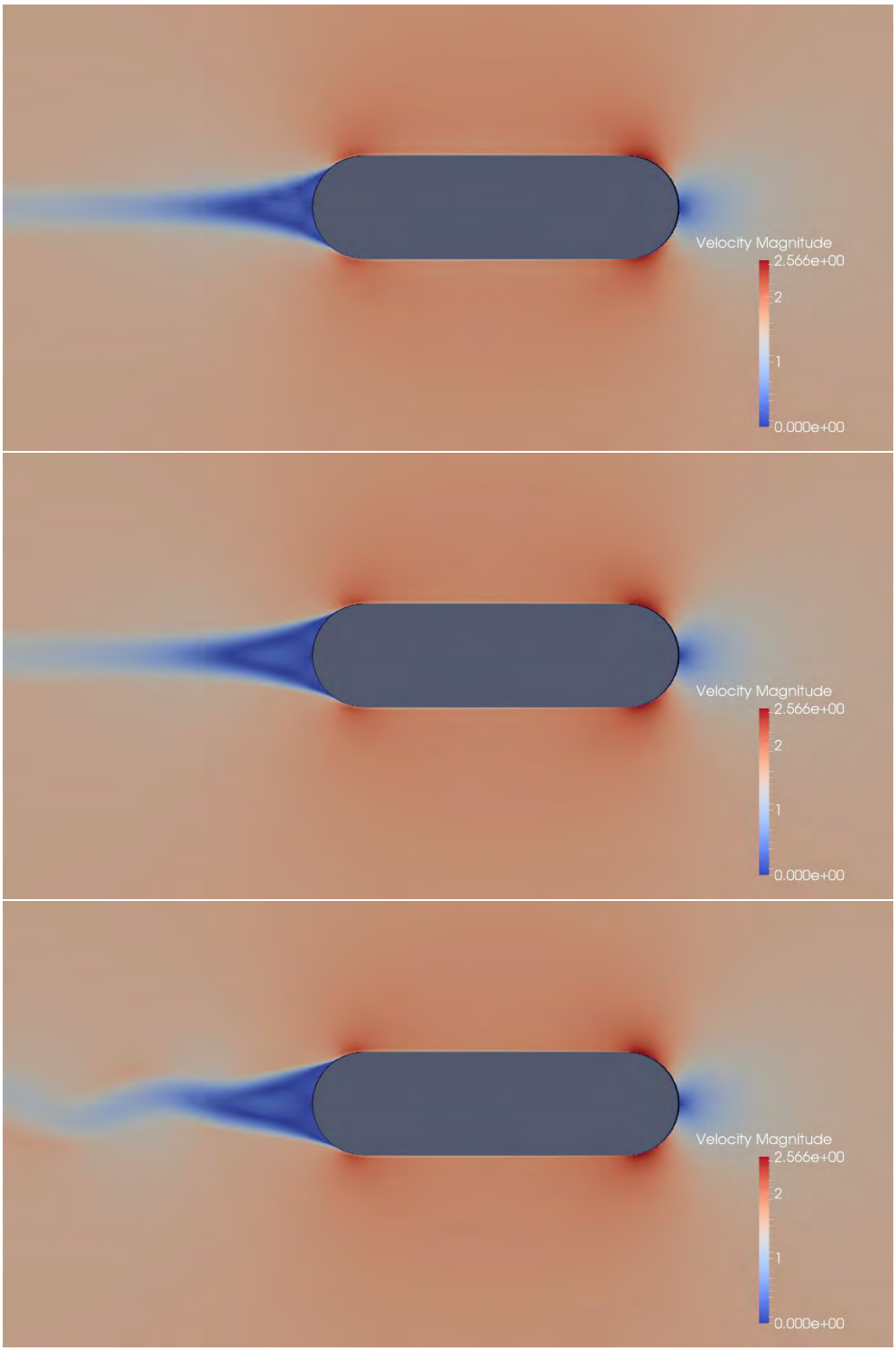

Figure 9 : Mesh convergence Mesh A, B and C (steady current 2D) (zoom) .

Although the Calculation are steady state there are some “instabilities” observed on the very fine mesh (Mesh C) (Figure 9). those instability may not reflect a real transient instability, the steady state calculation performed try to converge during iterations steps to find a steady solution, but in this case the solution for such mesh size show a not totally steady solution. We cannot extract useful information from this last picture as there is no time resolution information on the solution, been this

a steady state calculation. Future calculation could be expanded to 2D VIV checks. With transient calculation.

From this convergence study the main conclusion is that a mesh size close to MESH B can provide similar results in terms of drag compared to the more refined mesh C. The Average Mesh B size will be selected for the 3D final mesh

5.3 WALL ROUGHNESS STUDY.

3 wall roughness (0mm, 1mm and 5mm) are tested. For Mesh B and 0.25s time step.

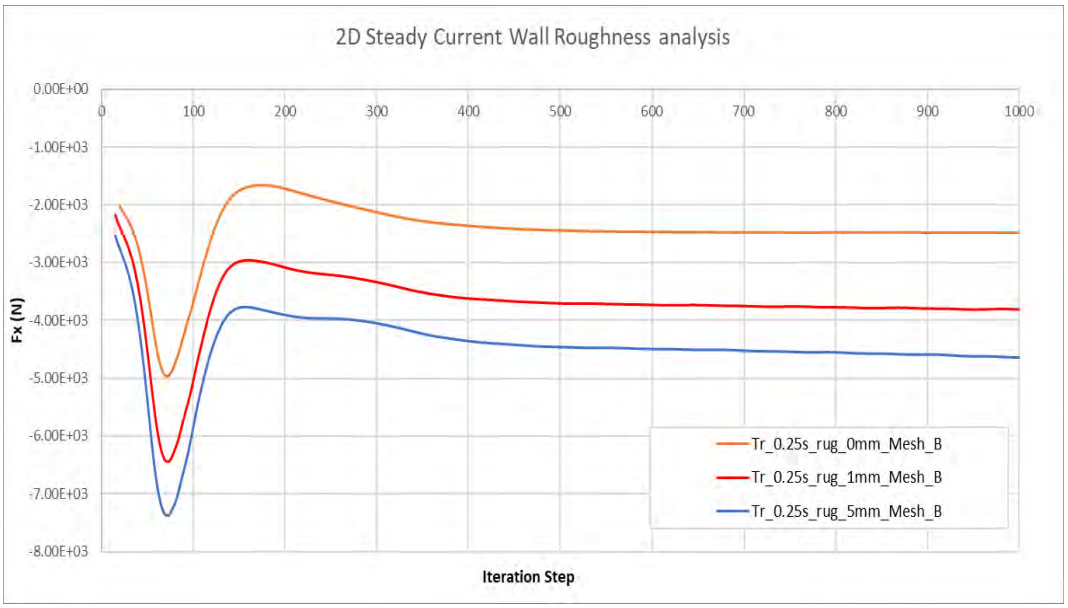

Figure 10 : Wall Roughness Study Mesh B and 0.25s.

It is observed, as expected, a significant influence of the wall roughness on the total resistance of the Pontoon. It has been decided to perform further calculation for 3D cases with 1mm roughness, representing a small roughness on the surface. From previous graph it is observed the following approx. relation regrading roughness influence.

Wall roughness	Resistance increase
0mm	100%
1mm	154%
5mm	187%

Table 4 : Increase of resistance between smooth surface and rough wall

Those values are preliminary as they are calculated for a 2D section and not fully converged rough wall solution.

5.4 2D KC ITERATION SENSITIVITY.

Two cases are tested for 5 and 10 iteration for each time step during transient simulation for KC study.

Mesh B is used and 0.25s time step.

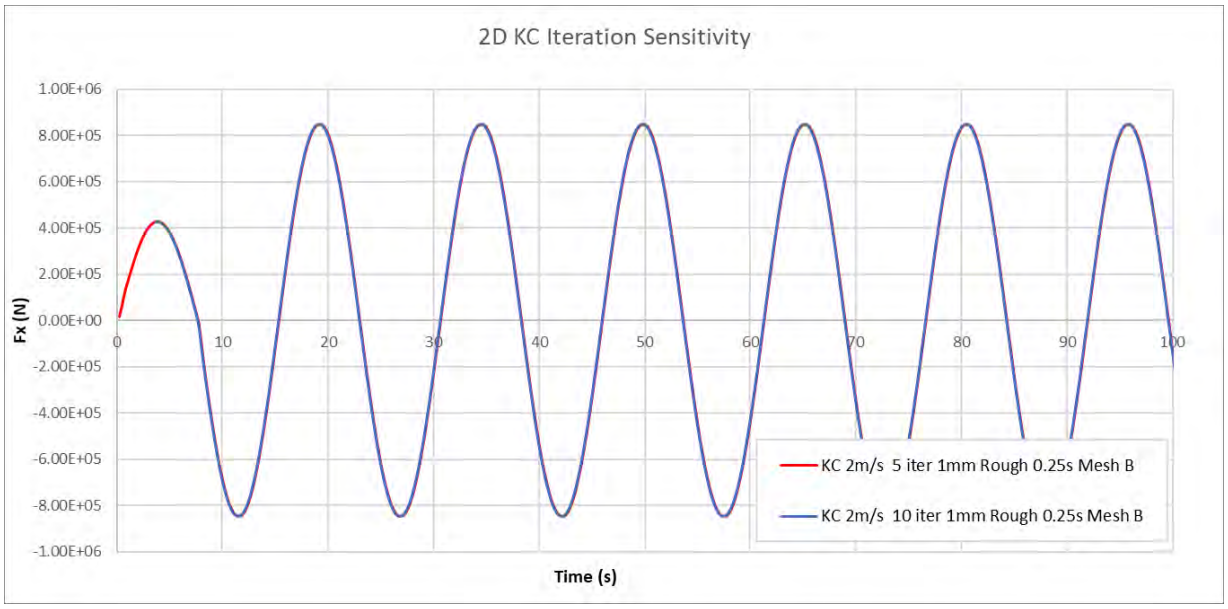

Figure 11 : Iteration Sensitivity results 2D mesh B

It is observed no significant difference for 5 and 10 iterations. 5 iteration will be sued for KC study

5.5 2D STUDY CONCLUSION

After Analysing the 2D Results the following decision are taken:

A 3D mesh density close to 2D mesh Case B is selected, resulting in an approx. 5.5Million Structured Hexahedral Elements 3D Mesh is generated.

The CFD model has the following characteristics

- Fix model (no sink and trim).
- Multi-Phase VOF Solver (solving only water phase, no free surface)
- Steady State Calculation (Current). Time step 0.25s
- KC Transient calculation. Time step 0.25s 5 iterations per time step (other Time step tested at section 5.1)
- Specified velocity at inlet/outlet corresponding to current speed or KC oscillations.
- Lateral top and bottom Walls, Fee slipping walls with no roughness.
- Turbulence model: SST.
- Hull wall, No slip wall, with 1mm roughness Water Density 1025 kg/m^3
- Kinematic Viscosity 1.04E-06 m2/s

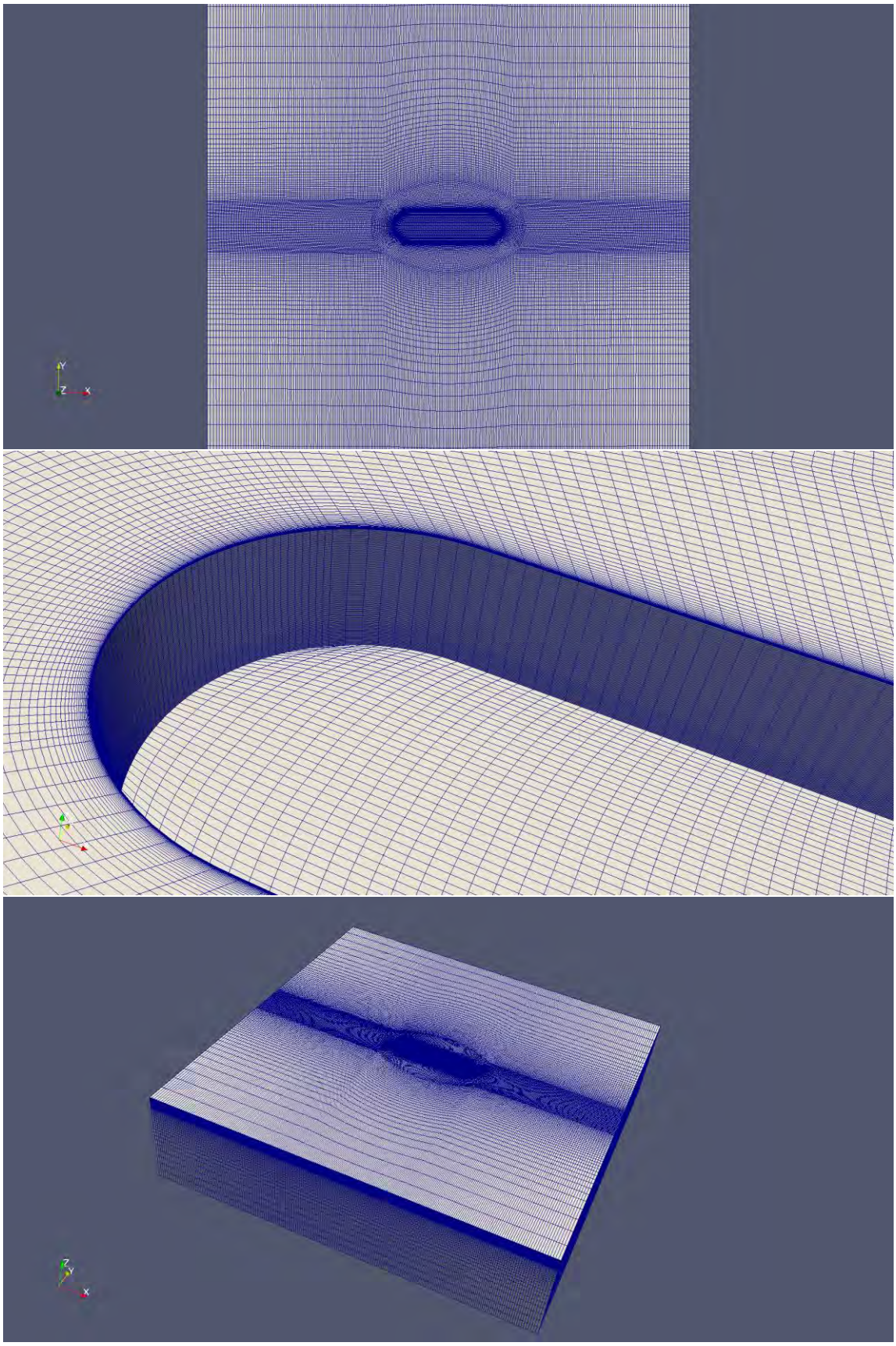

Figure 12 :Final Mesh used for the study 5.5 Million Elements

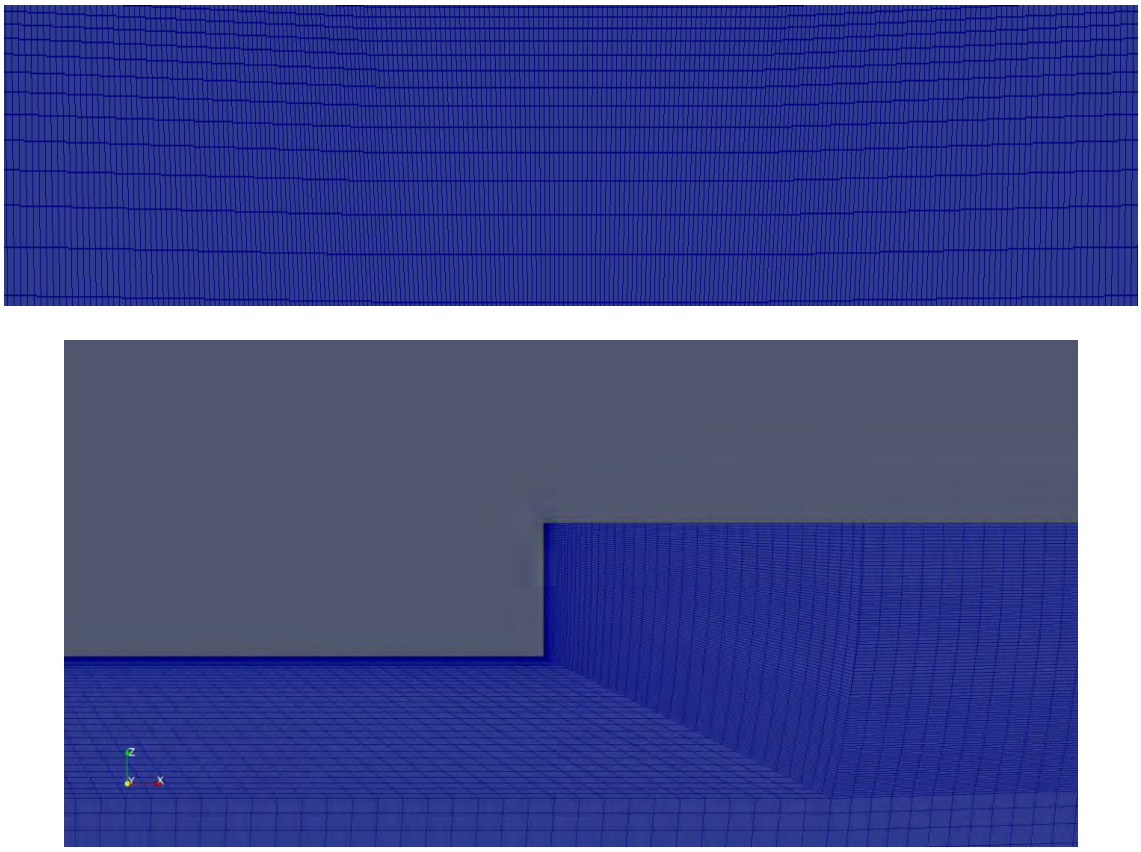

Figure 13 :Front View Cut (Y=0 Plane) of Final Mesh.

5.6 3D STEADY CURRENT RESULTS

A steady current of 3knots is applied “going to” X negative.

Different headings are applied 0, 15, 30 and 90 deg Heading. Heading relative to x-axis such that 0 deg is head current and 90 deg is beam current.

Result are postprocessed integrating over the whole hull and over section defined previously, see Figure 2

HULL1	HULL2	HULL3	HULL4	HULL5	HULL_bot	Total Force	Total Force
kN	kN	kN	kN	kN	kN	kN	Tonne

0deg 3kts	Fx	-7.3	-7.4	-7.7	-8.1	-6.0	-1.0	-37.4	-3.8
	Fy	0.0	0.0	0.0	0.0	0.1	0.0	0.2	0.0
15 deg 3kts	Fx	-9.4	-9.6	-9.9	-9.9	-6.0	-2.0	-46.7	-4.8
	Fy	9.7	9.7	9.6	8.9	3.8	-0.3	41.4	4.2
30 deg 3kts	Fx	-22.7	-22.4	-21.8	-20.3	-10.1	-2.3	-99.6	-10.1
	Fy	25.7	26.0	25.6	23.0	10.9	-1.6	109.6	11.2
90 deg 3kts	Fx	-72.8	-71.2	-68.8	-63.4	-41.7	0.6	-317.3	-32.3
	Fy	0.0	0.0	0.0	0.0	0.0	0.6	0.6	0.1

Table 5 : Sectional Loads for steady current

Y direction lateral and X direction longitudinal. Assuming a drag Coefficient Cd based on classical aerodynamic formulation the following Drag coefficient are obtained for 0deg Heading and steady current.

$$Fdrag = \frac{1}{2}\rho \cdot Cd \cdot A \cdot V^2$$

Ro: water density= 1025 kg/m^3

A= frontal Area = 14.9 m^2 (per section)

V= Current Speed = 1.5432 m/s

Kinematic Viscosity m2/s 1.00E-06

Cd	HULL1	HULL2	HULL3	HULL4	HULL5
0deg 3kts	0.40	0.41	0.42	0.44	0.33

Table 6 : Drag Coef for =deg Steady Current

Drag and Lift coef can be obtained for different heading but all depending on Client frame of reference and formulation used on his time domain code. Once we understand how the client will use those data (orcaflex modelling) we could provide consistent formulation for Drag an lift depending on hull frame of reference or world frame of reference.

The local frame used for calculations is shown on previous picture. The point 0 is the Floater centre (X=0, Y=0) and it is at the free surface (Z=0).

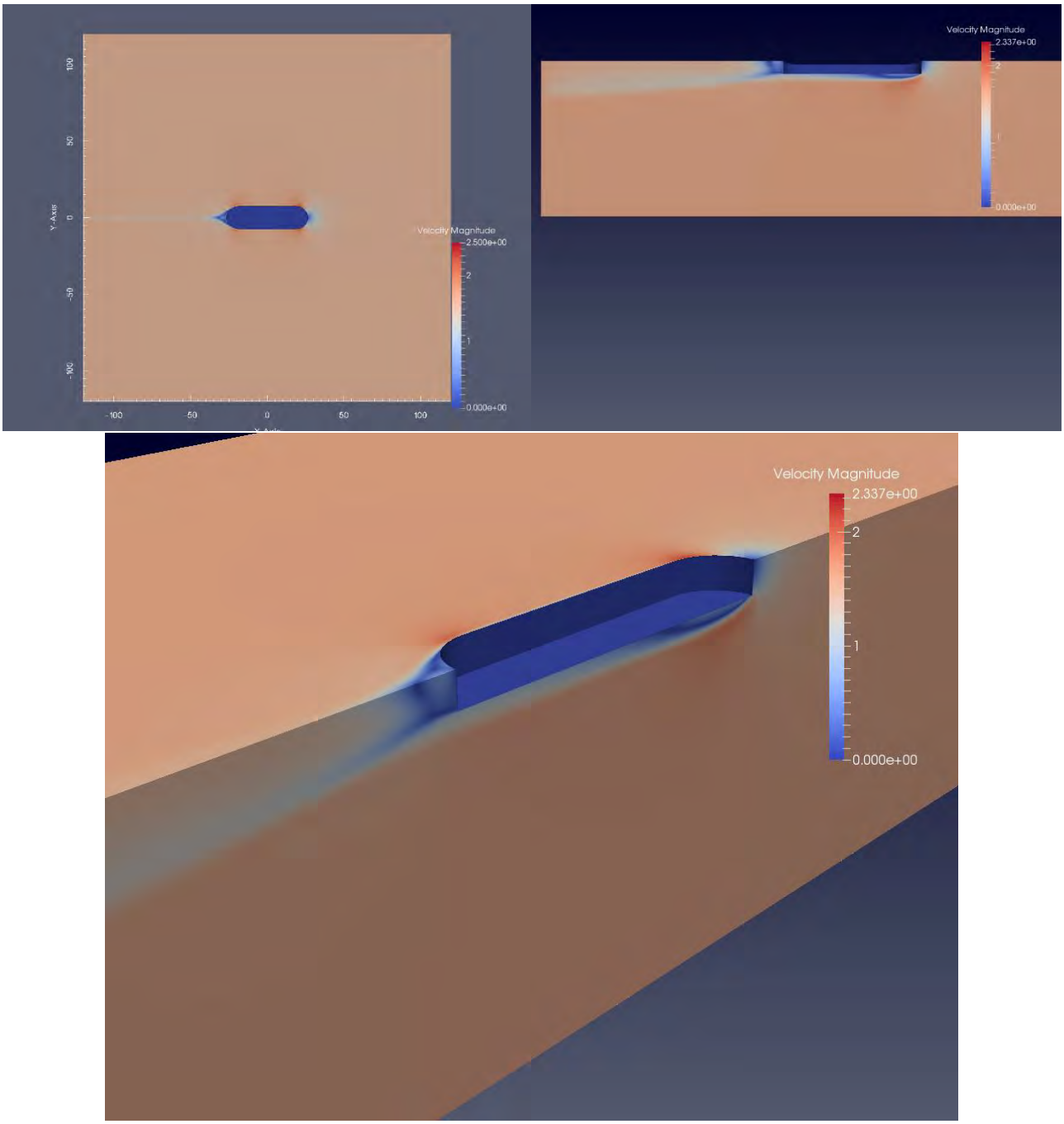

Figure 14 : 0 deg Velocity plot

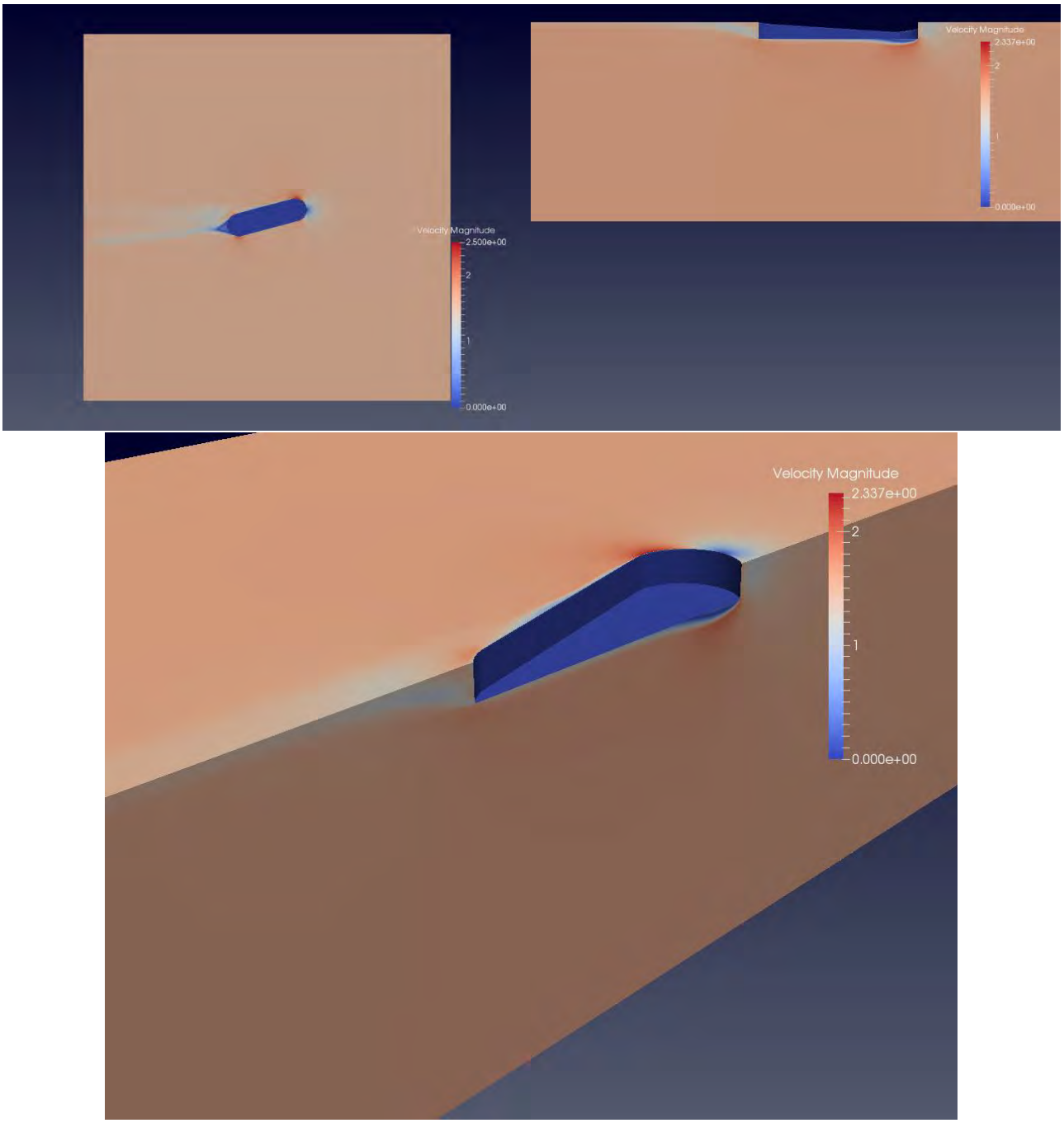

Figure 15 : 15 deg Velocity plot

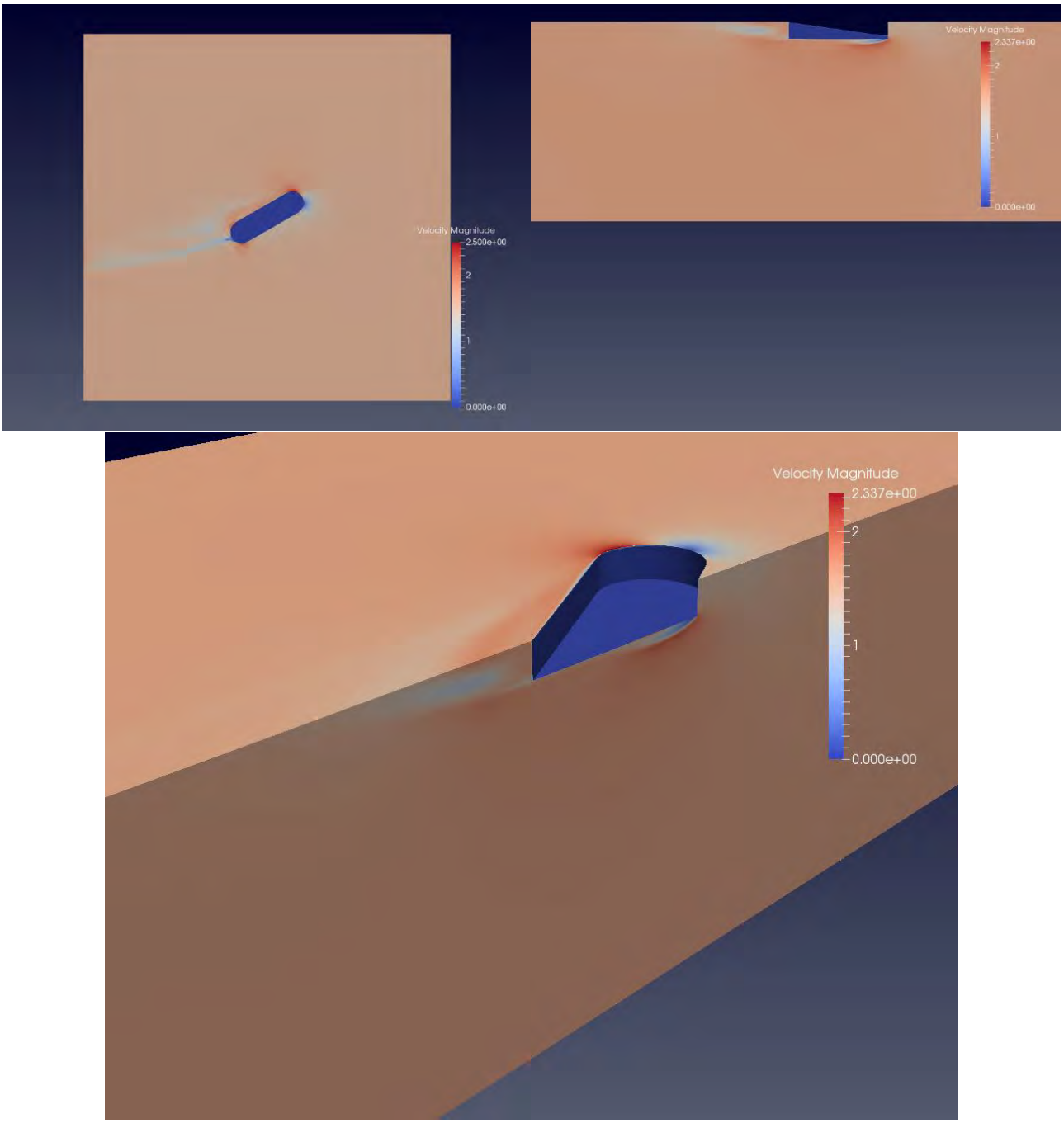

Figure 16 : 30 deg Velocity plot

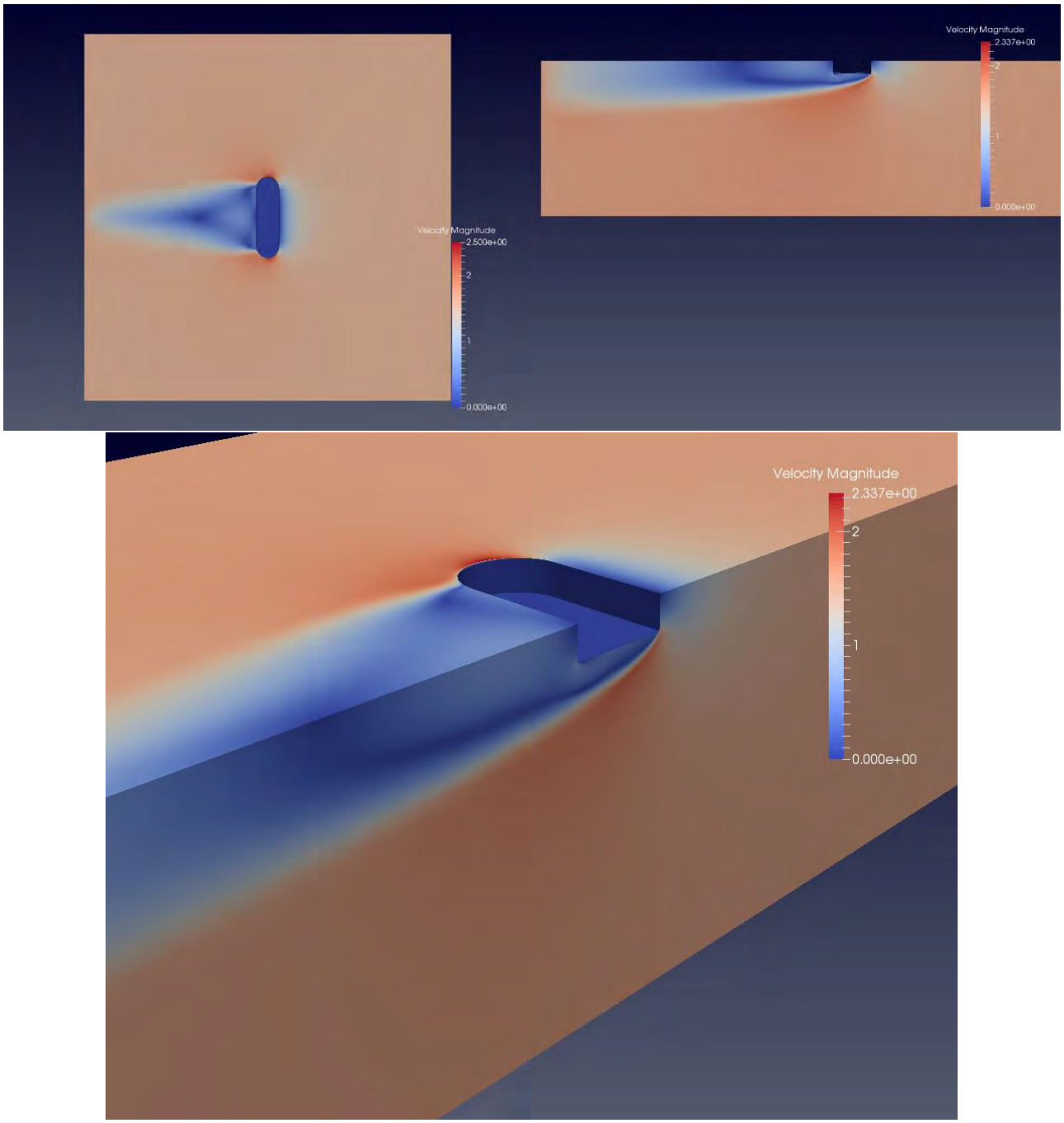

Figure 17 : 90 deg Velocity plot

1.2 KC STUDY

A KC (Keulegan-Carpenter) study is performed to understand the behaviour of the fix structure under oscillatory fluid flow.

$$K_C = \frac{V T}{L},$$

T= oscillation period (for motion or waves)

V= Amplitude of Velocity of oscillation.

L= Characteristics length. In this study MULTICONSULT selected the transverse direction of the hull14.9m to be the characteristic length

The heading is 0deg and the period of the oscillatory flow is fixed at 15s.

With the previous inputs the following test matrix has been agreed with the client.

T	Oscillation Period	s	15.0	15.0	15.0	15.0	15.0
w	Oscillation Freq	s	0.419	0.419	0.419	0.419	0.419
L	Characteristic length	m	14.9	14.9	14.9	14.9	14.9
Kc			0.50	1.00	2.00	3.00	4.00
V	fluid oscillation vel Amplitude	m/s	0.5	0.99	1.99	2.98	3.97

Table 7 : Test Matrix for KC cases

The model uses the same mesh as previous calculation with the only difference of the inlet and outlet water speed is based on an oscillatory time function.

5.6.1 Process to calculate Added mass and damping values.

It is assumed that a harmonic relative velocity signal corresponds to an equivalent harmonic motion on the structure on a steady fluid; This is a common assumption based on experimental data acquired by oscillatory U tanks (moving fluid) or by forced oscillation test (moving floater).

In the following figure it is plot a generated signal of position velocity and acceleration of a harmonic motion, the velocity signa is the input to velocity at inlet and outlet during CFD simulation. A ramp to provide a soft starting on CFD simulation is added during simulation. (from second 0 to 7.5) not shown in the following figure

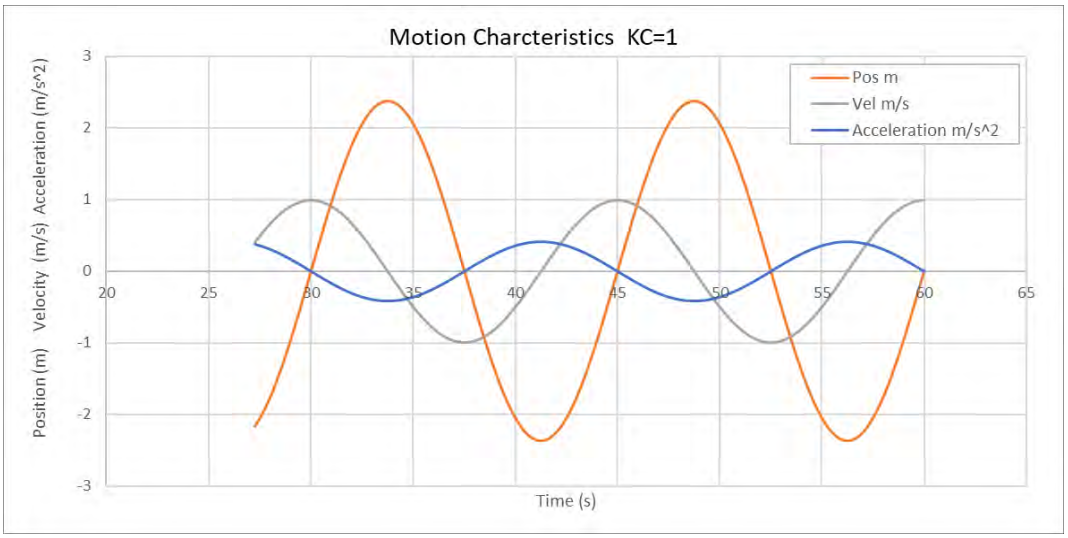

Figure 18 : Example of Position Velocity and Acceleration Synthetic signal

The CFD simulation provides a Force X signal for the complete structure and for the previous section discretized during mesh generation.

The theoretical acceleration signal is used as input to calculated phase between acceleration and forces.

The X force signal is adjusted by an harmonic signal. (1st order harmonic signal)

Acceleration signal: $A(t) = a \cdot w^2 \cdot \cos(wt)$

Force Signal: $Fx(t) = Ft \cdot \cos(wt + \varphi)$

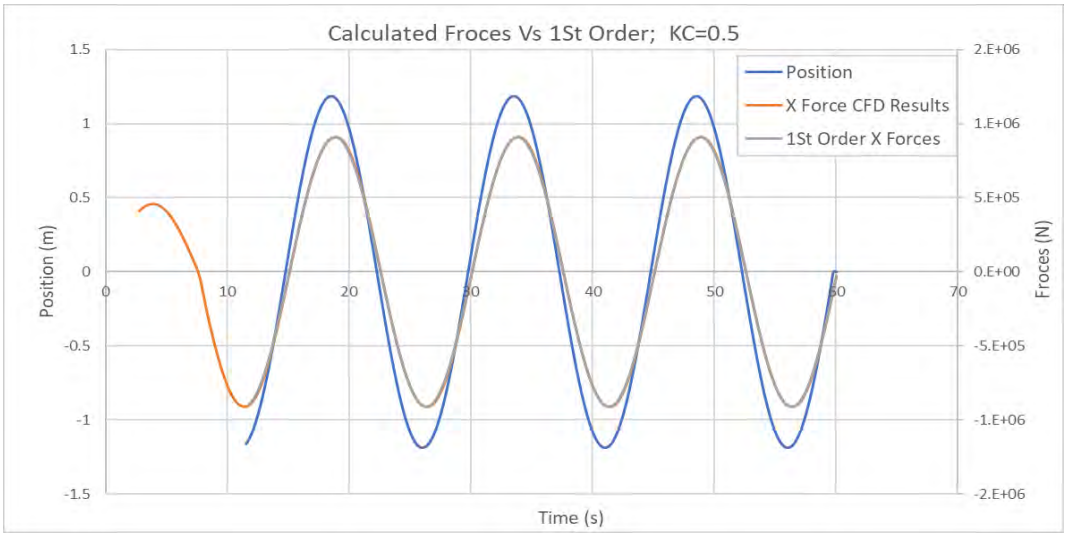

Figure 19 : CFD signal and fitted 1st order harmonic function.

The amplitude of force is directly calculated from CFD fx signal (averaged over positive and negative peaks)

The phase is calculated by adjusting mean square error method between synthetic signal and CFD X force signal.

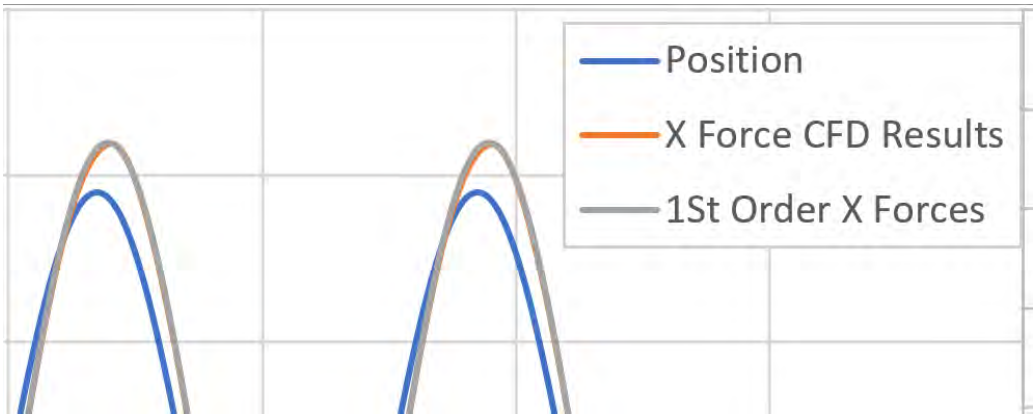

Figure 20 : Fitness of X force CFD signal (orange) with synthetic harmonic signal (grey) Phase calculated by minimising RMS error between both signals

Once calculated the amplitude and phase of the 1st order signal, the higher order error (difference between 1st order generated signal and CFD calculated results) can be calculated for observation and future discussion.

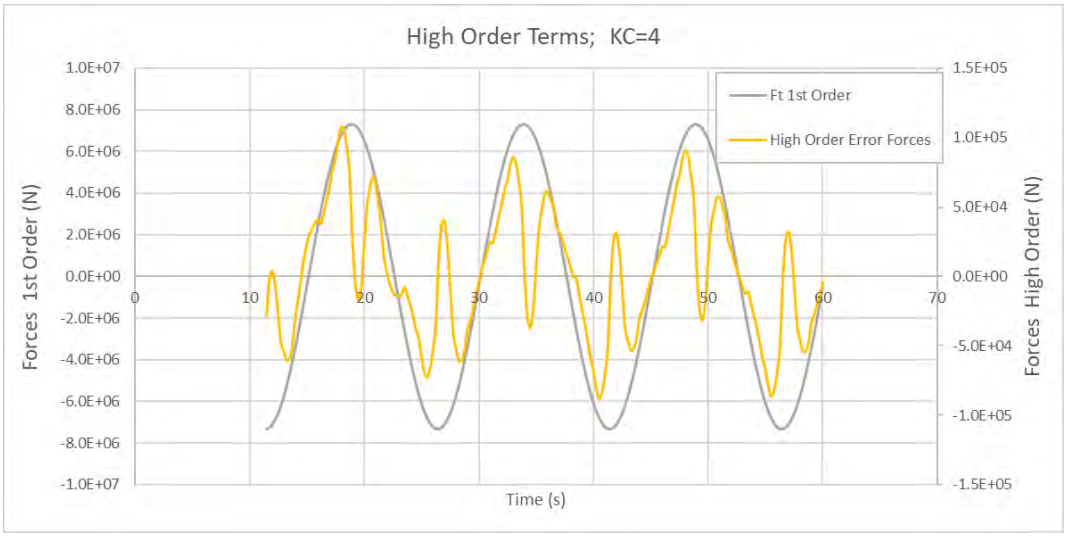

Figure 21 : 1st order Fitted Signal (grey) and High order signal (Orange, amplified scale): difference between 1st order and CFD resultant forces. (different scale both signals)

The final force signal can also be defined as a composition of force in phase with acceleration (added mass) and forces in phase with velocity (damping or viscous terms)

$$Fx(t) = Fi \cdot \cos(wt) + Fv \cdot sen(wt)$$

Doing a calculation at wt =0 and wt =pi/2 it can be calculated the Fi and Fv amplitudes values.

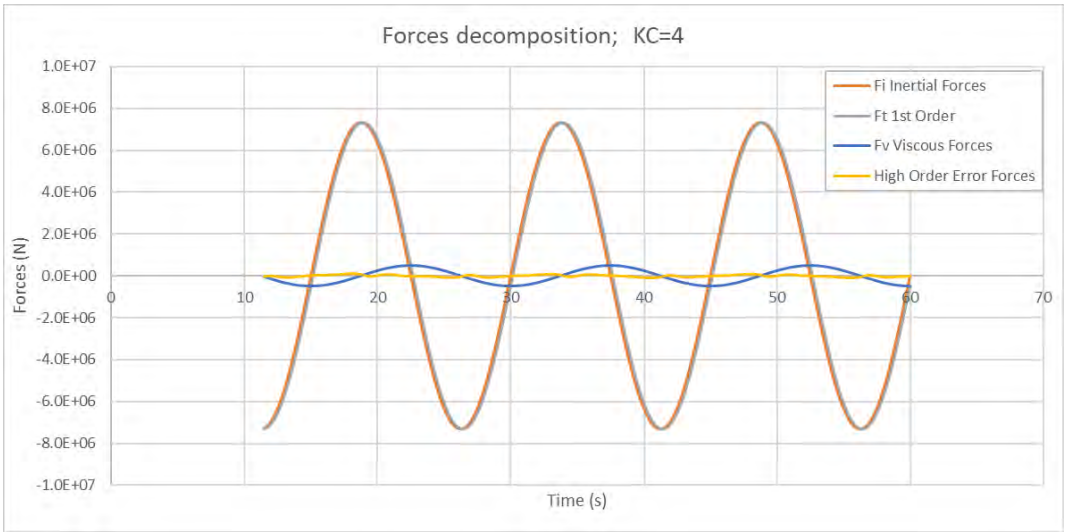

Figure 22: Inertial and viscous terms derived signals.

With those values the Added mass is directly calculated as Fi/(acceleration amplitude) and Damping term is Fv/(velocity amplitude).

Added mass coef Ca is defined in this study from: Finertial= Total Mass·acceleration. = (Mass+Added Mass)*Acceleration. Been Mass (the displacement of the pontton).

Total Forces; KC=4	
Phase (deg)	-3.82
F total Amplitude 1s Order (N)	7.32E+06
F inertia amplitude (N)	7.31E+06
F viscous amplitude (N)	4.88E+05
Second Order Force Amplitude RMS (N)	4.59E+04
Mass (t)	3803.0
Added Mass (t)	589.0
Damping (kN/(m/s))	123.0

Table 8 : Result Example for Full Pontoon and KC = 4

Similar procedure is performed for the 5 section of the hull to calculate section drag and added mass coef.

Section Forces; KC=4	HULL1 Fx	HULL2 Fx	HULL3 Fx	HULL4 Fx	HULL5 Fx	HULL bott
Phase (deg)	-3.18	-3.33	-3.66	-4.21	-3.92	-67.24
F total Amplitude 1s Order (N)	1.48E+06	1.47E+06	1.47E+06	1.46E+06	1.44E+06	3.13E+04
F inertia amplitude (N)	1.47E+06	1.47E+06	1.46E+06	1.45E+06	1.44E+06	1.21E+04
F viscous amplitude (N)	8.18E+04	8.17E+04	8.14E+04	8.09E+04	7.98E+04	1.73E+03
Mass (t)	760.6	760.6	760.6	760.6	760.6	0.0
Added Mass (t)	124.7	123.1	119.5	113.6	102.5	7.3

Damping (kN/(m/s))	20.6	20.6	20.5	20.4	20.1	0.4

Table 9 : Result Example for Pontoon sections and KC = 4

The results comparing Section and full pontoon shows a small dependency of the section position on Ca and Cd.

In the following Section full detailed result are provided for the different KC number tested.

Full videos of the transient simulation are provided attached to this report.

5.6.2 KC = 0.5 Results

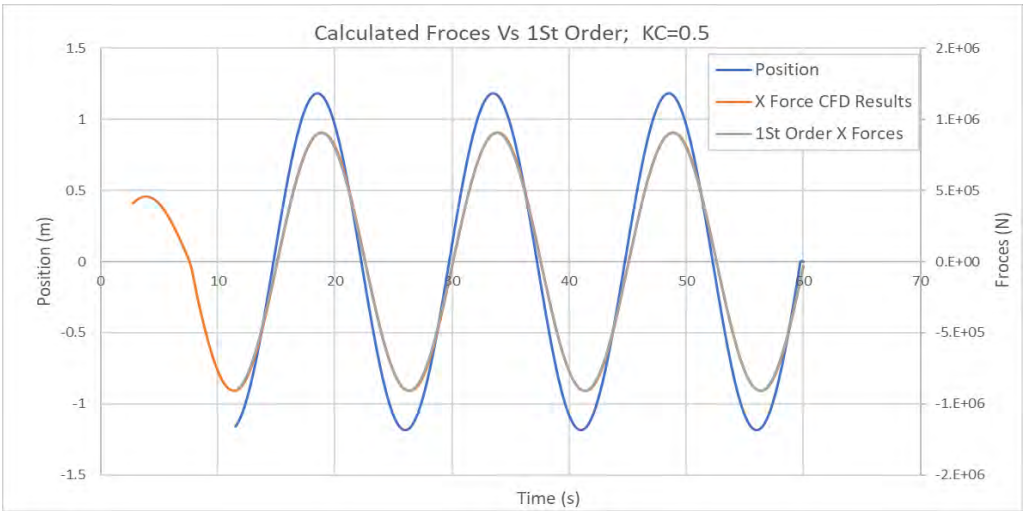

Figure 23: KC 0.5. CFD force Signal and 1st order fit

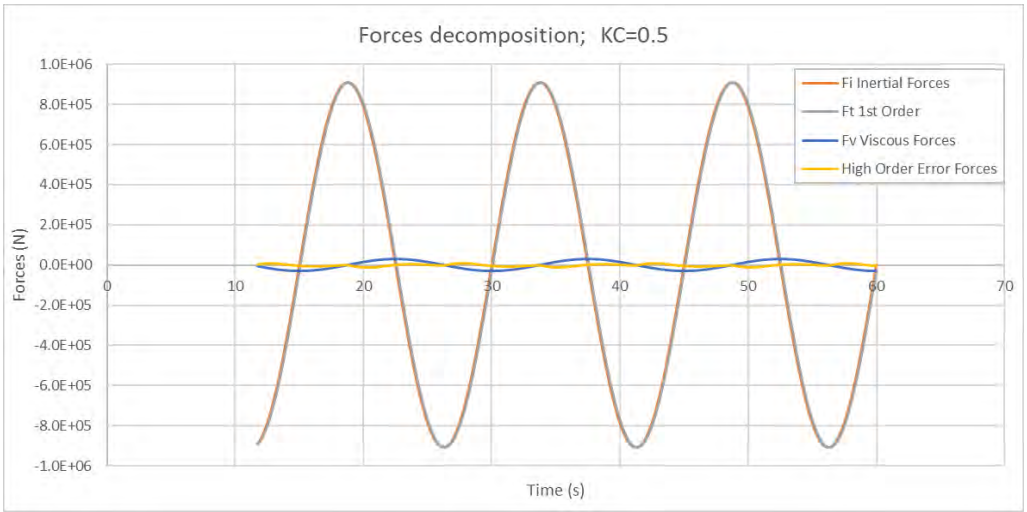

Figure 24: KC 0.5. Force Decomposition

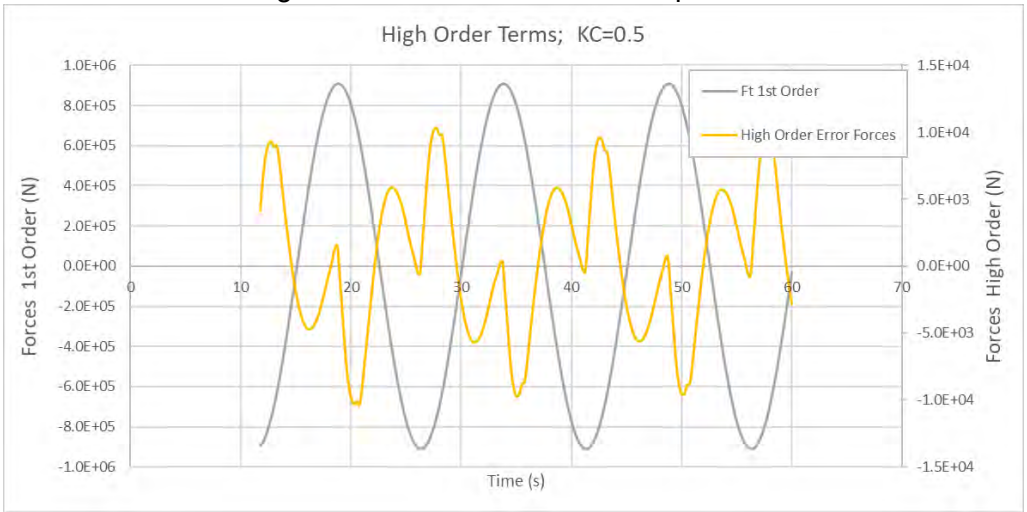

Figure 25: KC 0.5. 1st and High order terms

Total Forces; KC=0.5	
Phase (deg)	-1.93
F total Amplitude 1s Order (N)	9.09E+05
F inertia amplitude (N)	9.08E+05
F viscous amplitude (N)	3.06E+04
Second Order Force Amplitude RMS (N)	5.88E+03
Mass (t)	3803.0
Added Mass (t)	564.4
Damping (kN/(m/s))	61.6

Table 10 : Result Example for Pontoon; KC = 0.5

Section Forces; KC=0.5	HULL1 Fx	HULL2 Fx	HULL3 Fx	HULL4 Fx	HULL5 Fx	HULL bott
Phase (deg)	-3.33	-1.63	-1.69	-1.89	-2.63	-71.81
F total Amplitude 1s Order (N)	1.84E+05	1.83E+05	1.83E+05	1.81E+05	1.78E+05	1.02E+03
F inertia amplitude (N)	1.84E+05	1.83E+05	1.82E+05	1.81E+05	1.78E+05	3.17E+02
F viscous amplitude (N)	1.07E+04	1.06E+04	1.06E+04	1.05E+04	1.03E+04	5.89E+01
Mass (t)	760.6	760.6	760.6	760.6	760.6	0.0
Added Mass (t)	122.0	121.1	116.8	109.7	93.0	1.5
Damping (kN/(m/s))	21.5	21.4	21.3	21.2	20.8	0.1

Table 11 : Result Example for Pontoon Sections; KC = 0.5

5.6.3 KC = 1 Results

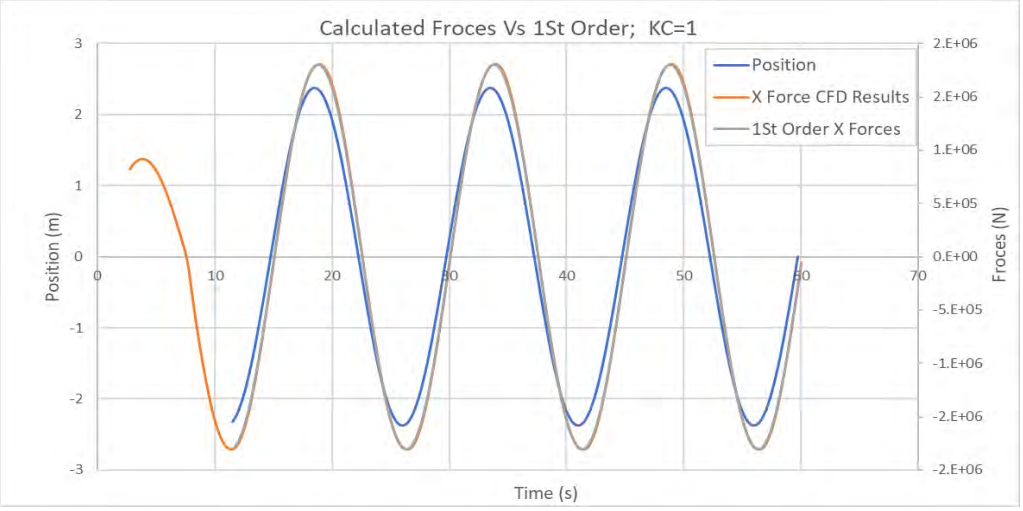

Figure 26: KC 1. CFD force Signal and 1st order fit

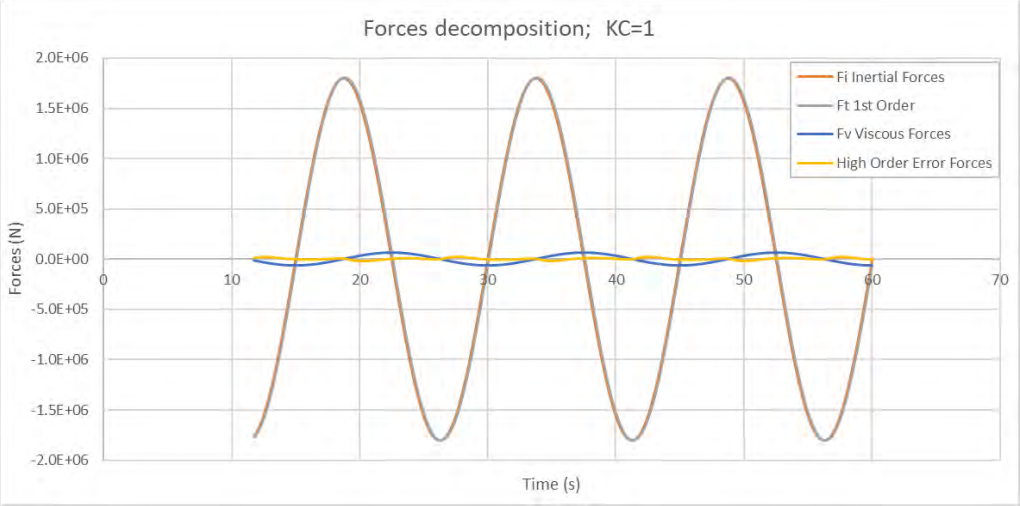

Figure 27: KC 1. Force Decomposition

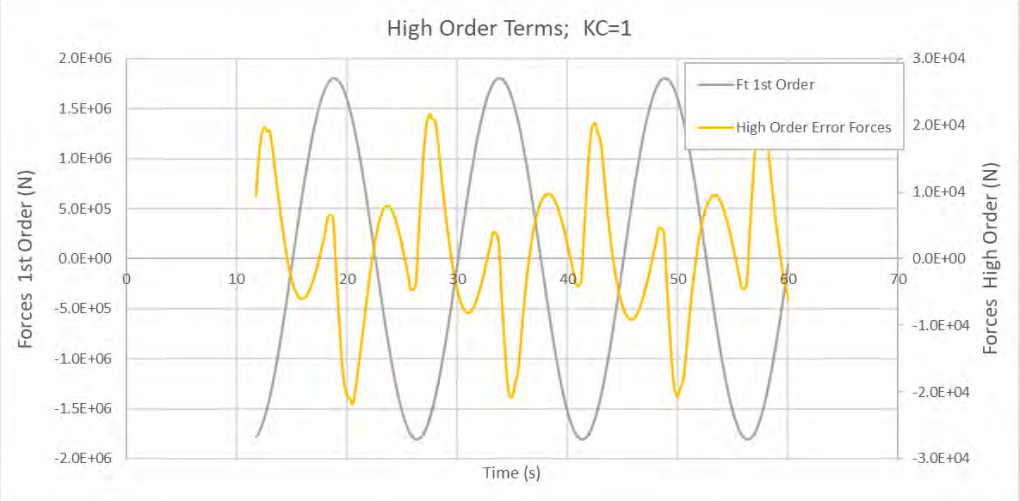

Figure 28: KC 1. 1st and High order terms

Total Forces; KC=1	
Phase (deg)	-2.02
F total Amplitude 1s Order (N)	1.80E+06
F inertia amplitude (N)	1.80E+06
F viscous amplitude (N)	6.35E+04
Second Order Force Amplitude RMS (N)	1.12E+04
Mass (t)	3803.0
Added Mass (t)	531.2
Damping (kN/(m/s))	64.0

Table 12 : Result Example for Pontoon; KC =1

Section Forces; KC=1	HULL1 Fx	HULL2 Fx	HULL3 Fx	HULL4 Fx	HULL5 Fx	HULL bott
Phase (deg)	-1.54	-1.61	-1.81	-2.25	-2.66	-69.90
F total Amplitude 1s Order (N)	3.65E+05	3.64E+05	3.62E+05	3.59E+05	3.53E+05	3.08E+03
F inertia amplitude (N)	3.65E+05	3.64E+05	3.62E+05	3.59E+05	3.52E+05	1.06E+03
F viscous amplitude (N)	9.81E+03	9.79E+03	9.75E+03	9.66E+03	9.49E+03	8.28E+01
Mass (t)	760.6	760.6	760.6	760.6	760.6	0.0
Added Mass (t)	116.5	114.5	110.1	102.5	86.8	2.5
Damping (kN/(m/s))	9.9	9.9	9.8	9.7	9.6	0.1

Table 13 : Result Example for Pontoon Sections; KC = 1

5.6.4 KC = 2 Results

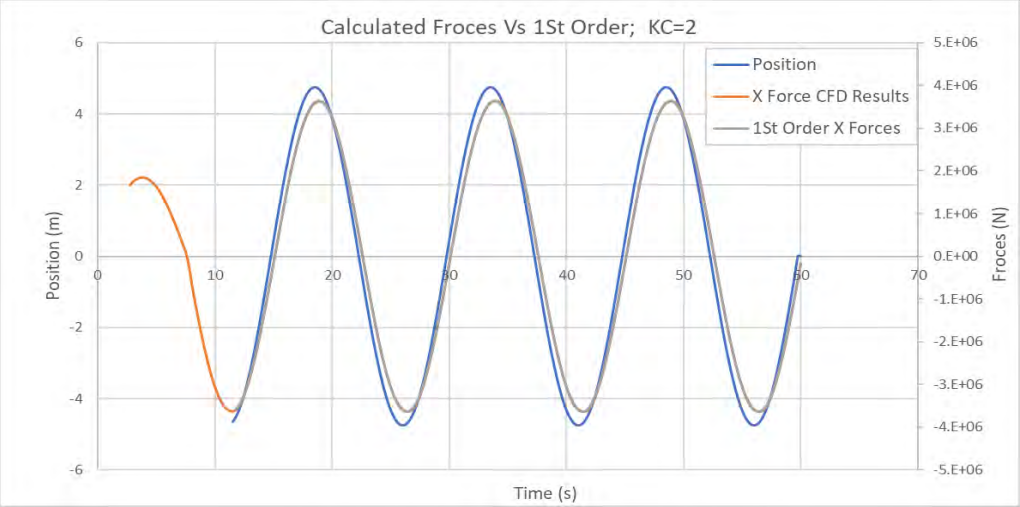

Figure 29: KC 2. CFD force Signal and 1st order fit

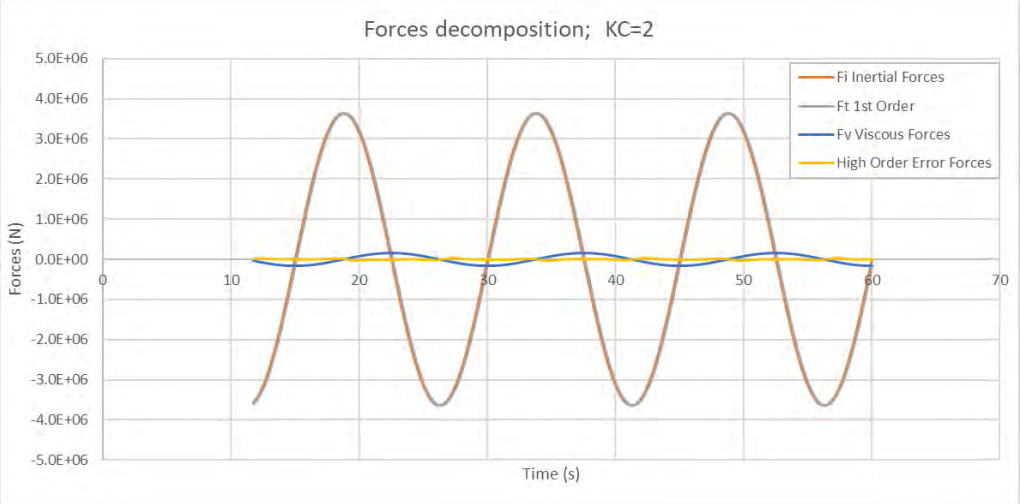

Figure 30: KC 2. Force Decomposition

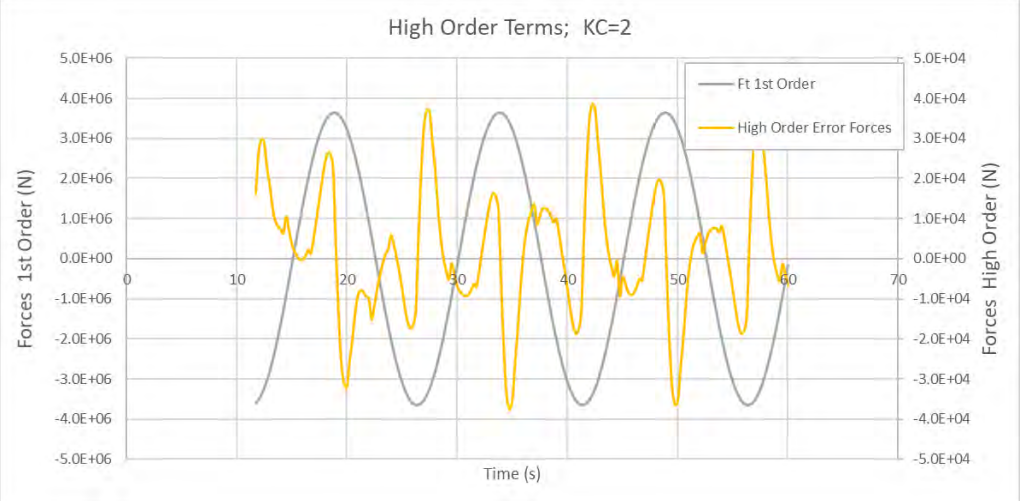

Figure 31: KC 2. 1st and High order terms

Total Forces; KC=2	
Phase (deg)	-2.54
F total Amplitude 1s Order (N)	3.64E+06
F inertia amplitude (N)	3.64E+06
F viscous amplitude (N)	1.62E+05
Second Order Force Amplitude RMS (N)	1.98E+04
Mass (t)	3803.0
Added Mass (t)	569.9
Damping (kN/(m/s))	81.4

Table 14 : Result Example for Pontoon; KC =2

Section Forces; KC=2	HULL1 Fx	HULL2 Fx	HULL3 Fx	HULL4 Fx	HULL5 Fx	HULL bott
Phase (deg)	-2.02	-2.13	-2.41	-2.94	-2.88	-68.78
F total Amplitude 1s Order (N)	7.36E+05	7.34E+05	7.31E+05	7.25E+05	7.13E+05	9.74E+03
F inertia amplitude (N)	7.36E+05	7.34E+05	7.30E+05	7.24E+05	7.12E+05	3.53E+03
F viscous amplitude (N)	2.59E+04	2.59E+04	2.57E+04	2.55E+04	2.51E+04	3.43E+02
Mass (t)	760.6	760.6	760.6	760.6	760.6	0.0
Added Mass (t)	123.7	121.7	117.2	109.2	95.2	4.2
Damping (kN/(m/s))	13.1	13.0	13.0	12.9	12.6	0.2

Table 15 : Result Example for Pontoon Sections; KC = 2

5.6.5 KC = 3 Results

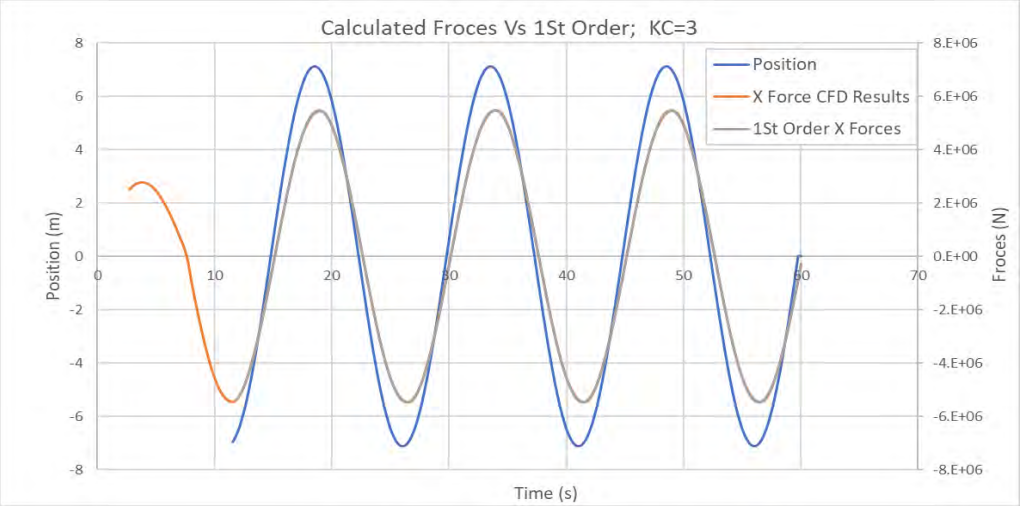

Figure 32: KC 3. CFD force Signal and 1st order fit

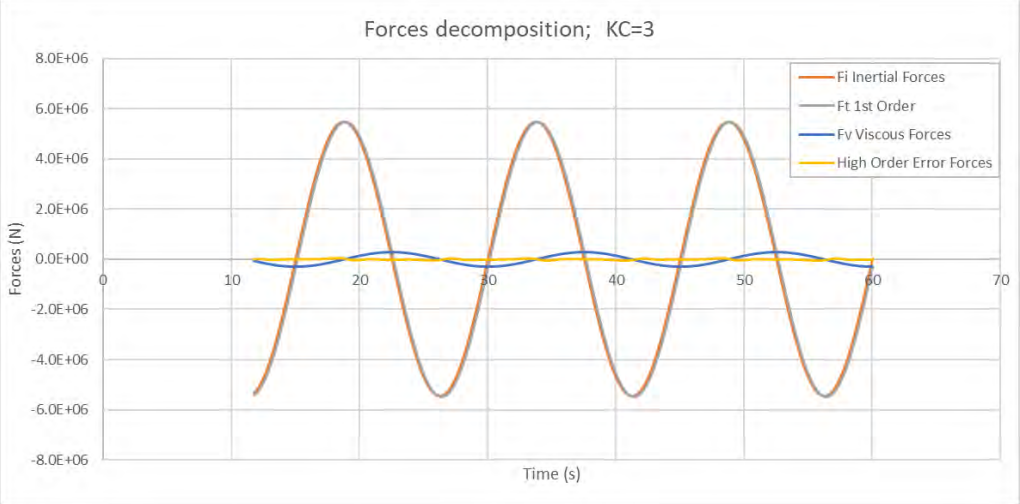

Figure 33: KC 3. Force Decomposition

Figure 34: KC 3. 1st and High order terms

Total Forces; KC=3	
Phase (deg)	-3.10
F total Amplitude 1s Order (N)	5.47E+06
F inertia amplitude (N)	5.46E+06
F viscous amplitude (N)	2.96E+05
Second Order Force Amplitude RMS (N)	3.19E+04
Mass (t)	3803.0
Added Mass (t)	575.7
Damping (kN/(m/s))	99.4

Table 16 : Result Example for Pontoon; KC =3

Section Forces; KC=3	HULL1 Fx	HULL2 Fx	HULL3 Fx	HULL4 Fx	HULL5 Fx	HULL bott
Phase (deg)	-2.56	-2.68	-2.97	-3.47	-3.26	-67.91
F total Amplitude 1s Order (N)	1.10E+06	1.10E+06	1.10E+06	1.09E+06	1.07E+06	1.92E+04
F inertia amplitude (N)	1.10E+06	1.10E+06	1.10E+06	1.09E+06	1.07E+06	7.21E+03
F viscous amplitude (N)	4.93E+04	4.92E+04	4.90E+04	4.86E+04	4.79E+04	8.56E+02
Mass (t)	760.6	760.6	760.6	760.6	760.6	0.0
Added Mass (t)	123.5	121.8	117.9	110.7	97.1	5.8
Damping (kN/(m/s))	16.6	16.5	16.5	16.3	16.1	0.3

Table 17 : Result Example for Pontoon Sections; KC = 3

5.6.6 KC = 4 Results

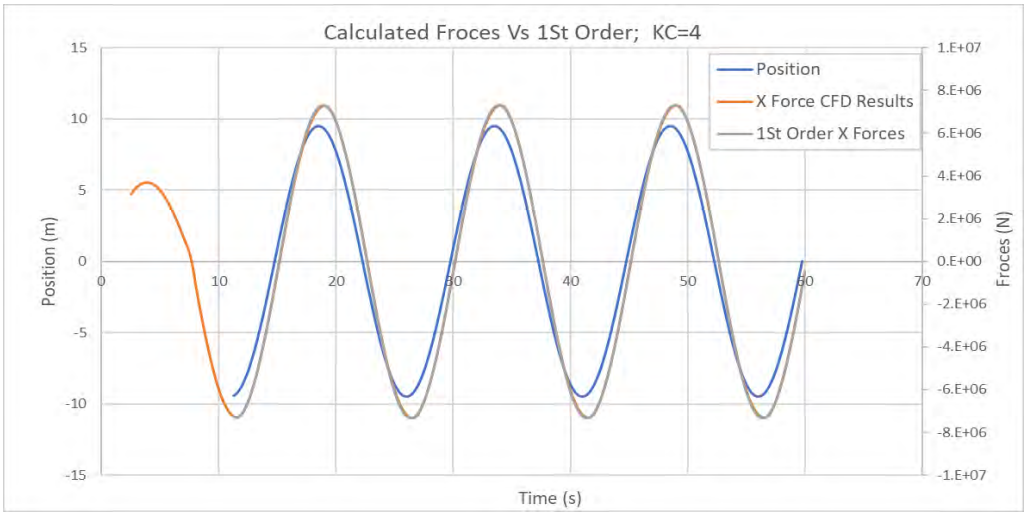

Figure 35: KC 4. CFD force Signal and 1st order fit

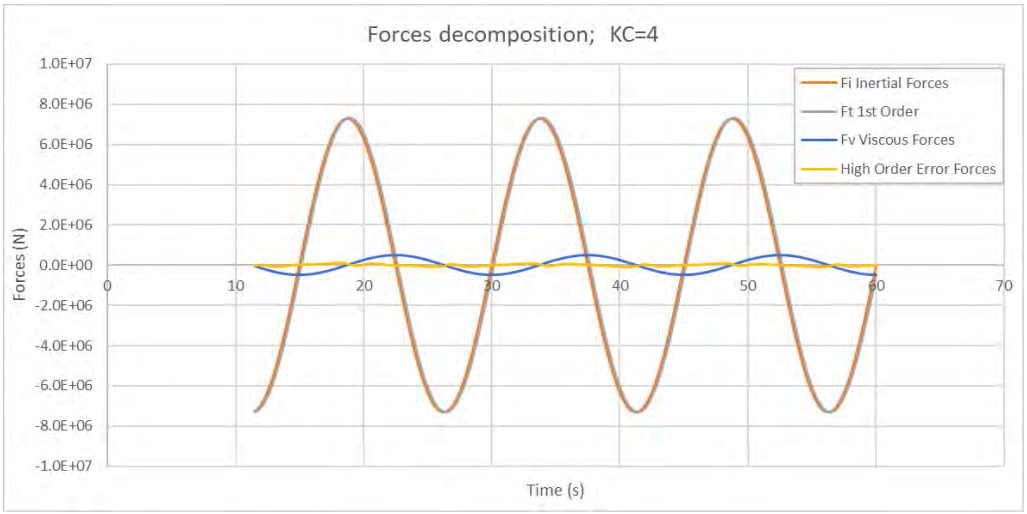

Figure 36: KC 4. Force Decomposition

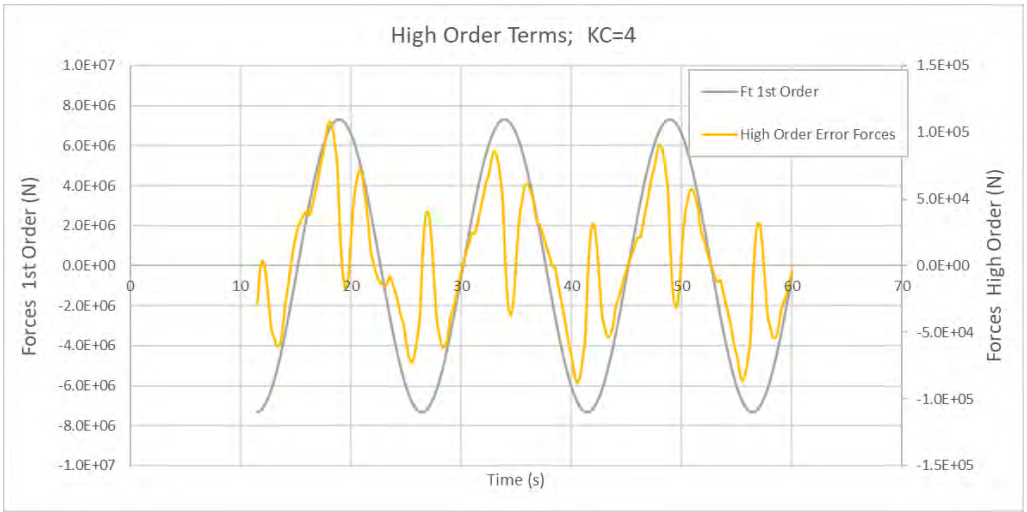

Figure 37: KC 4. 1st and High order terms

Total Forces; KC=4	
Phase (deg)	-3.82
F total Amplitude 1s Order (N)	7.32E+06
F inertia amplitude (N)	7.31E+06
F viscous amplitude (N)	4.88E+05
Second Order Force Amplitude RMS (N)	4.59E+04
Mass (t)	3803.0
Added Mass (t)	589.0
Damping (kN/(m/s))	123.0

Table 18 : Result Example for Pontoon; KC =4

Section Forces; KC=4	HULL1 Fx	HULL2 Fx	HULL3 Fx	HULL4 Fx	HULL5 Fx	HULL bott
Phase (deg)	-3.18	-3.33	-3.66	-4.21	-3.92	-67.24
F total Amplitude 1s Order (N)	1.48E+06	1.47E+06	1.47E+06	1.46E+06	1.44E+06	3.13E+04
F inertia amplitude (N)	1.47E+06	1.47E+06	1.46E+06	1.45E+06	1.44E+06	1.21E+04
F viscous amplitude (N)	8.18E+04	8.17E+04	8.14E+04	8.09E+04	7.98E+04	1.73E+03
Mass (t)	760.6	760.6	760.6	760.6	760.6	0.0
Added Mass (t)	124.7	123.1	119.5	113.6	102.5	7.3
Damping (kN/(m/s))	20.6	20.6	20.5	20.4	20.1	0.4

Table 19 : Result Example for Pontoon Sections; KC = 4

6 ADDITIONAL KC CASES

Additional KC with different velocity amplitude and frequencies are requested 6 June 2019.

			Previously Calculated Cases					Additionally Calculated Cases				
	CASE Identificatory		KC 0.5	KC 1	KC 2	KC 3	KC 4	KC 1B	KC 1C	KC 2B	KC 1D	KC 20
T	Oscillation Period	s	15.0	15.0	15.0	15.0	15.0	8.0	25.0	8.0	15.0	30.0
w	Oscillation Freq	rad/s	0.419	0.419	0.419	0.419	0.419	0.785	0.251	0.785	0.419	0.209
L	Characteristic length	m	14.9	14.9	14.9	14.9	14.9	14.9	14.9	14.9	14.9	14.9
Kc	Keulegan Karpenter Nº		0.5	1.0	2.0	3.0	4.0	1.0	1.0	2.0	1.0	20.0
V	fluid oscillation vel Amplitude	m/s	0.500	0.990	1.990	2.980	3.970	1.870	0.595	3.725	0.990	9.935
V std	Current Constant	m/s	0	0	0	0	0	0	0	0	1	0
	Added Mass	t	564	544	561	574	591	592	527	602	549	606
	Damping	kN/(m/s)	62	64	81	99	123	185	31	216	65	194

Table 20 : Total KC cases calculated and main results. (blue new cases)

6.1.1 KC 1B Results

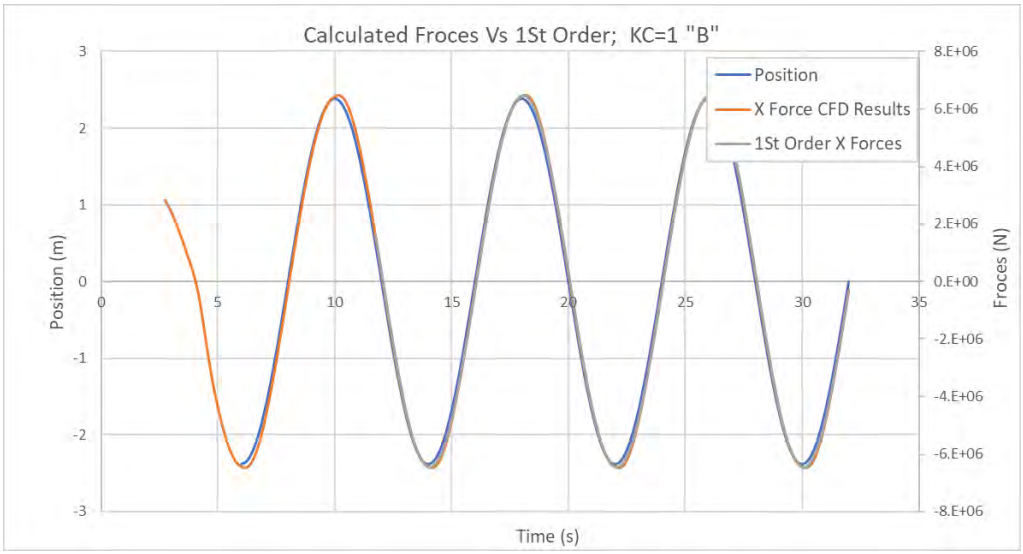

Figure 38: KC 1B. CFD force Signal and 1st order fit

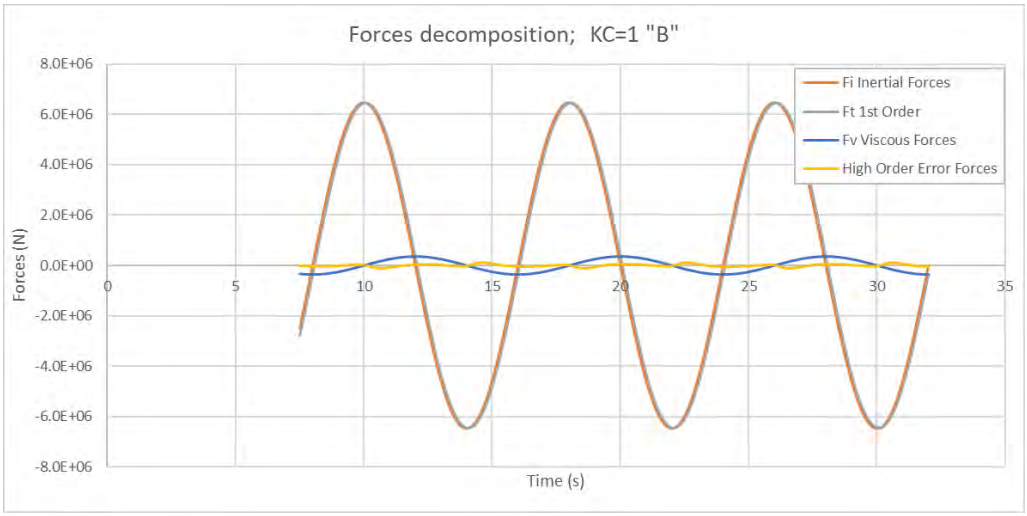

Figure 39: KC 1B. Force Decomposition

Figure 40: KC 1B. 1st and Higher order terms (different scales)

Total Forces; KC=1 "B"	
Phase (deg)	-3.06
F total Amplitude 1s Order (N)	6.46E+06
F inertia amplitude (N)	6.45E+06
F viscous amplitude (N)	3.45E+05
Second Order Force Amplitude RMS (N)	5.73E+04
Mass (t)	3803.0
Added Mass (t)	591.8
Damping (kN/(m/s))	184.6

Table 21 : Result Example for Pontoon; KC 1B

Section Forces; KC=1 "B"	HULL1 Fx	HULL2 Fx	HULL3 Fx	HULL4 Fx	HULL5 Fx	HULL bott
Phase (deg)	-2.52	-2.53	-2.71	-3.16	-3.68	-69.98
F total Amplitude 1s Order (N)	1.31E+06	1.30E+06	1.30E+06	1.29E+06	1.27E+06	1.05E+04
F inertia amplitude (N)	1.30E+06	1.30E+06	1.30E+06	1.29E+06	1.27E+06	3.60E+03
F viscous amplitude (N)	5.74E+04	5.72E+04	5.70E+04	5.66E+04	5.57E+04	4.62E+02
Mass (t)	760.6	760.6	760.6	760.6	760.6	0.0
Added Mass (t)	127.4	125.5	121.6	114.6	101.2	2.5
Damping (kN/(m/s))	30.7	30.6	30.5	30.2	29.8	0.2

Table 22 : Result Example for Pontoon Sections; KC 1B

6.1.2 KC 1C Results

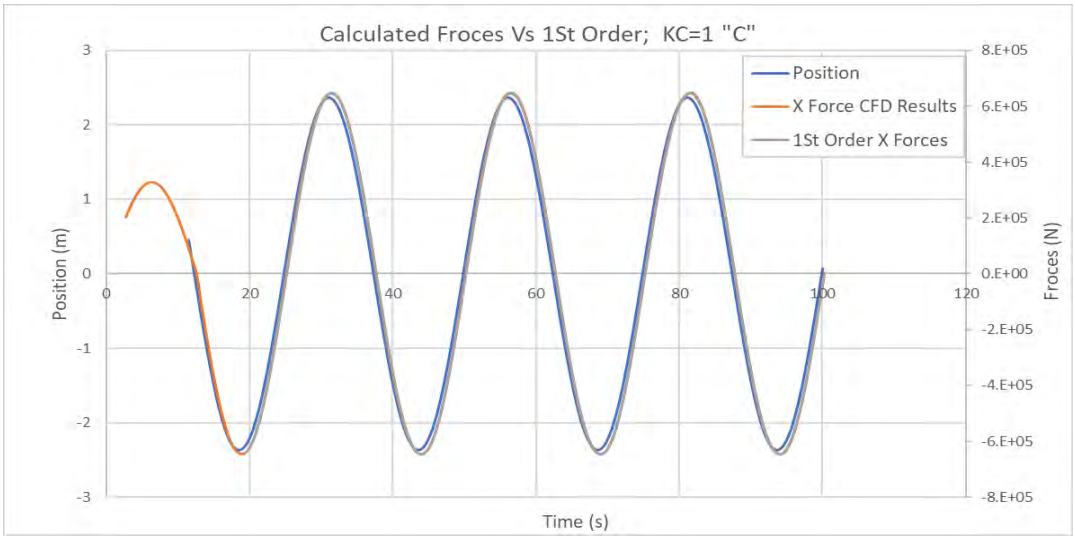

Figure 41: KC 1C. CFD force Signal and 1st order fit

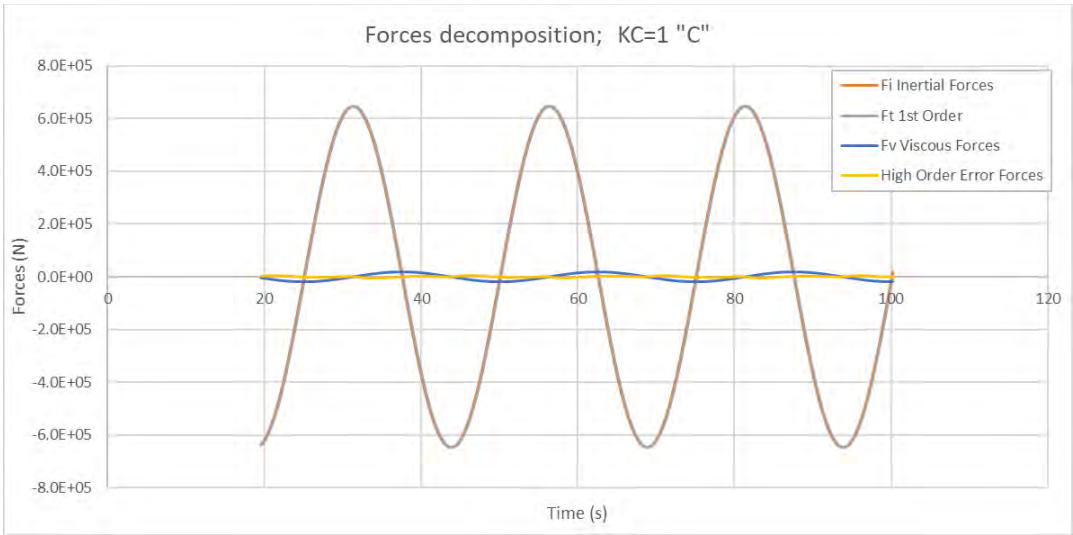

Figure 42: KC 1C. Force Decomposition

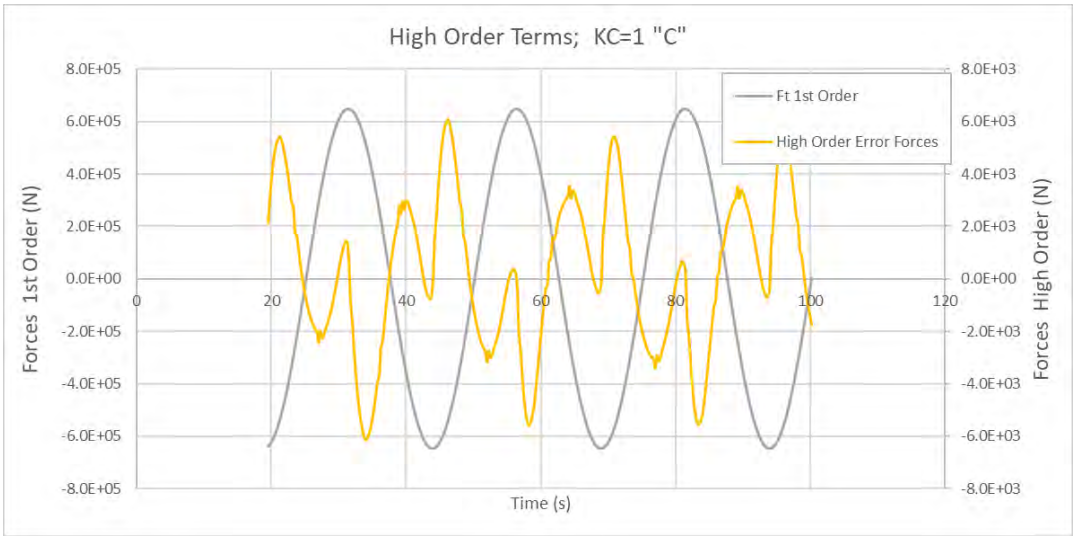

Figure 43: KC 1C. 1st and Higher order terms (different scales)

Total Forces; KC=1 "C"	
Phase (deg)	-1.64
F total Amplitude 1s Order (N)	6.47E+05
F inertia amplitude (N)	6.47E+05
F viscous amplitude (N)	1.85E+04
Second Order Force Amplitude RMS (N)	3.11E+03
Mass (t)	3803.0
Added Mass (t)	527.3
Damping (kN/(m/s))	31.1

Table 23 : Result Example for Pontoon; KC 1C

Section Forces; KC=1 "C"	HULL1 Fx	HULL2 Fx	HULL3 Fx	HULL4 Fx	HULL5 Fx	HULL bott
Phase (deg)	-1.07	-1.14	-1.33	-1.76	-2.12	-68.69
F total Amplitude 1s Order (N)	1.31E+05	1.31E+05	1.30E+05	1.29E+05	1.26E+05	1.14E+03
F inertia amplitude (N)	1.31E+05	1.31E+05	1.30E+05	1.29E+05	1.26E+05	4.13E+02
F viscous amplitude (N)	2.44E+03	2.44E+03	2.42E+03	2.40E+03	2.36E+03	2.12E+01
Mass (t)	760.6	760.6	760.6	760.6	760.6	0.0
Added Mass (t)	116.4	114.4	109.9	101.3	85.8	2.8
Damping (kN/(m/s))	4.1	4.1	4.1	4.0	4.0	0.0

Table 24 : Result Example for Pontoon Sections; KC 1C

6.1.3 KC 1D Results (KC with Constant Current Imposed)

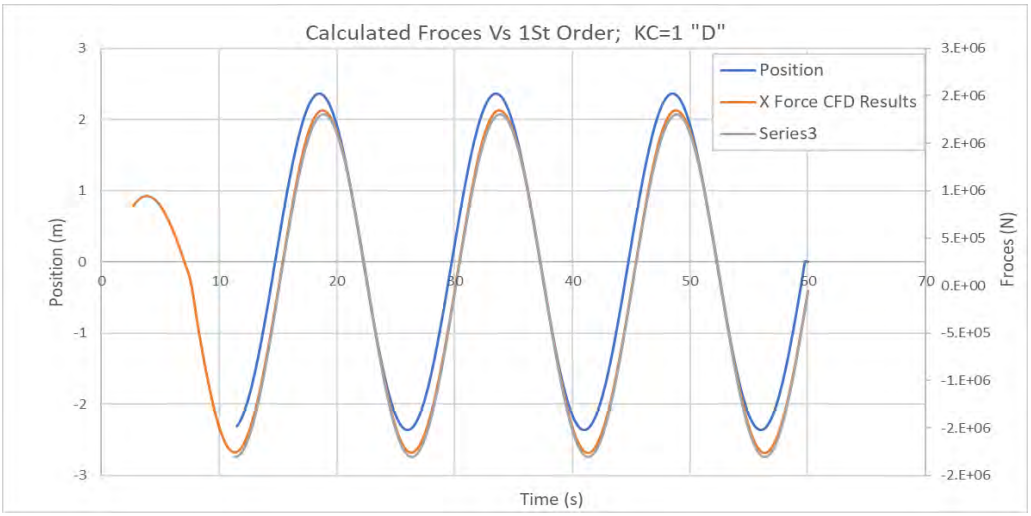

Figure 44: KC 1D. CFD force Signal and 1st order fit

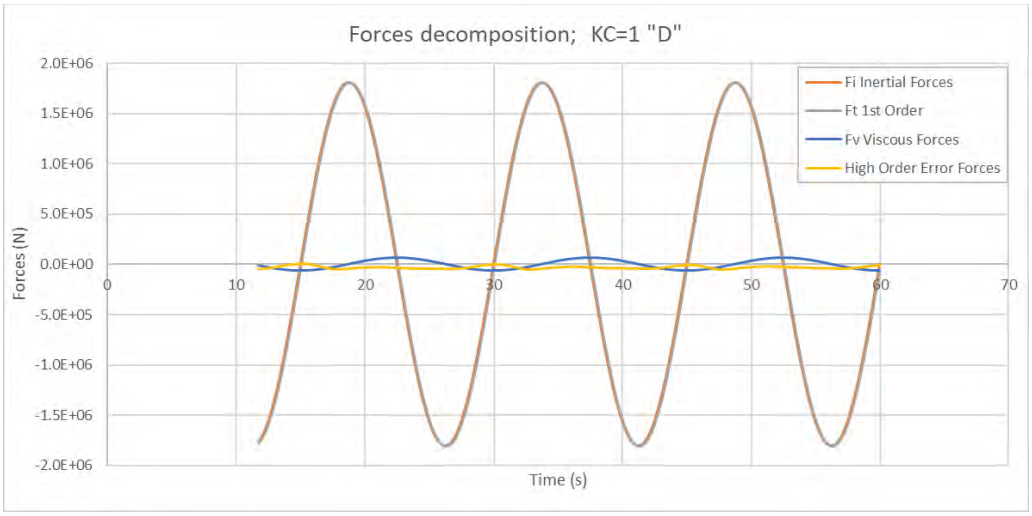

Figure 45: KD 1C. Force Decomposition

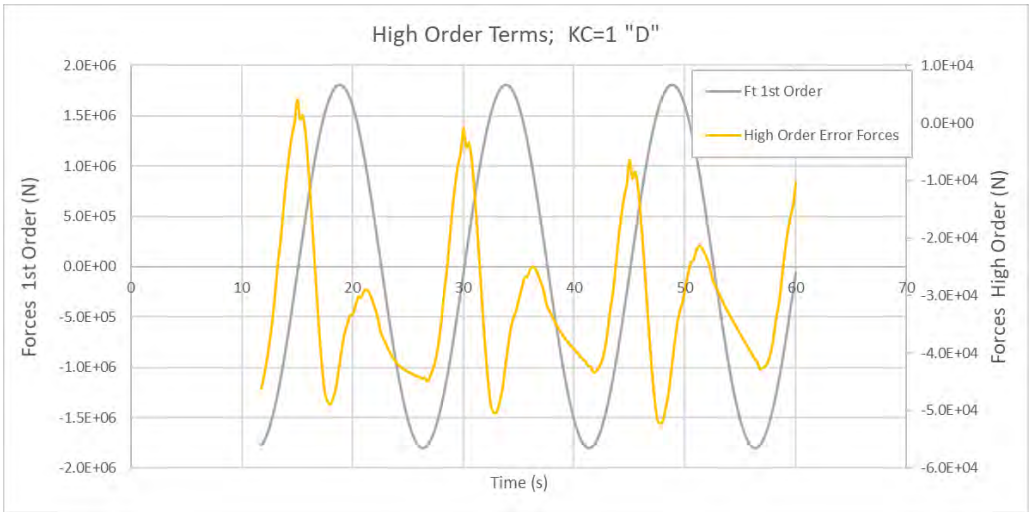

Figure 46: KC 1D. 1st and Higher order terms (different scales)

Total Forces; KC=1 "D"	
Phase (deg)	-2.04
F total Amplitude 1s Order (N)	1.81E+06
F inertia amplitude (N)	1.80E+06
F viscous amplitude (N)	6.42E+04
Second Order Force Amplitude RMS (N)	3.40E+04
Mass (t)	3803.0
Added Mass (t)	549.2
Damping (kN/(m/s))	64.8

Table 25 : Result Example for Pontoon; KC 1D

Section Forces; KC=1 "D"	HULL1 Fx	HULL2 Fx	HULL3 Fx	HULL4 Fx	HULL5 Fx	HULL bott
Phase (deg)	-1.79	-1.83	-1.92	-2.10	-1.93	-73.43
F total Amplitude 1s Order (N)	3.66E+05	3.65E+05	3.63E+05	3.59E+05	3.52E+05	3.74E+03
F inertia amplitude (N)	3.66E+05	3.65E+05	3.63E+05	3.59E+05	3.52E+05	1.07E+03
F viscous amplitude (N)	1.14E+04	1.14E+04	1.13E+04	1.12E+04	1.10E+04	1.17E+02
Mass (t)	760.6	760.6	760.6	760.6	760.6	0.0
Added Mass (t)	121.6	119.3	114.4	104.7	88.4	2.6
Damping (kN/(m/s))	11.6	11.5	11.5	11.3	11.1	0.1

Table 26 : Result Example for Pontoon Sections; KC 1D

6.1.4 KC 2B Results

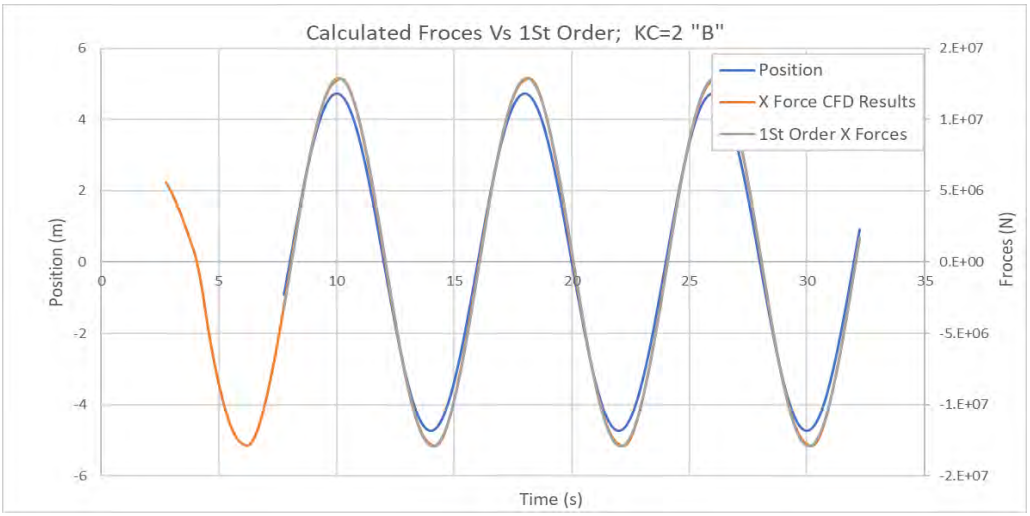

Figure 47: KC 2B. CFD force Signal and 1st order fit

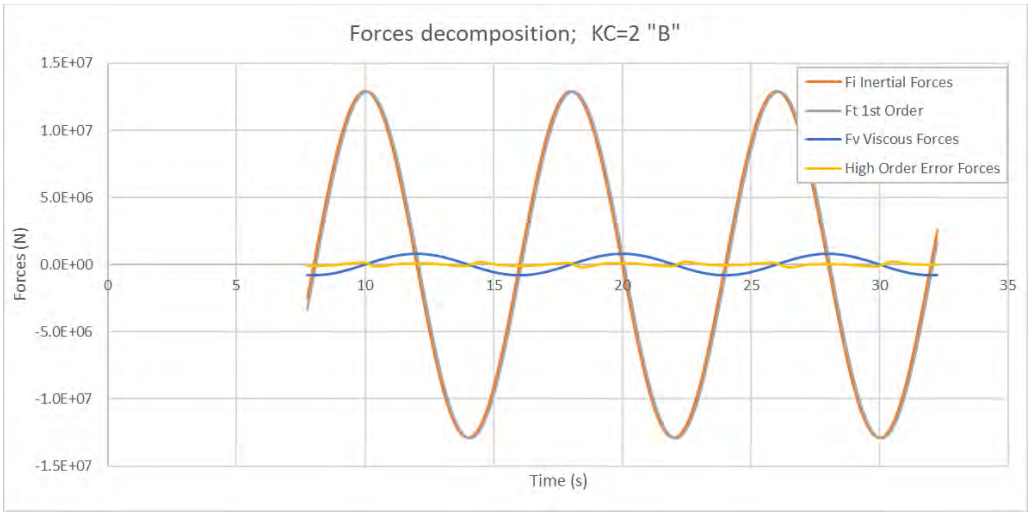

Figure 48: KC 2B. Force Decomposition

Figure 49: KC 2B. 1st and Higher order terms (different scales)

Total Forces; KC=2 "B"	
Phase (deg)	-3.57
F total Amplitude 1s Order (N)	1.291E+07
F inertia amplitude (N)	1.289E+07
F viscous amplitude (N)	8.03E+05
Second Order Force Amplitude RMS (N)	9.05E+04
Mass (t)	3803.0
Added Mass (t)	601.5
Damping (kN/(m/s))	215.6

Table 27 : Result Example for Pontoon; KC 2B

Section Forces; KC=2 "B"	HULL1 Fx	HULL2 Fx	HULL3 Fx	HULL4 Fx	HULL5 Fx	HULL bott
Phase (deg)	-2.92	-3.04	-3.33	-3.93	-4.00	-69.16
F total Amplitude 1s Order (N)	2.61E+06	2.60E+06	2.59E+06	2.57E+06	2.53E+06	3.27E+04
F inertia amplitude (N)	2.60E+06	2.60E+06	2.59E+06	2.57E+06	2.53E+06	1.16E+04
F viscous amplitude (N)	1.33E+05	1.33E+05	1.32E+05	1.31E+05	1.29E+05	1.67E+03
Mass (t)	760.6	760.6	760.6	760.6	760.6	0.0
Added Mass (t)	129.0	127.2	123.1	116.2	103.7	4.0
Damping (kN/(m/s))	35.7	35.6	35.4	35.2	34.7	0.4

Table 28 : Result Example for Pontoon Sections; KC 2B

6.1.5 KC 20 Results

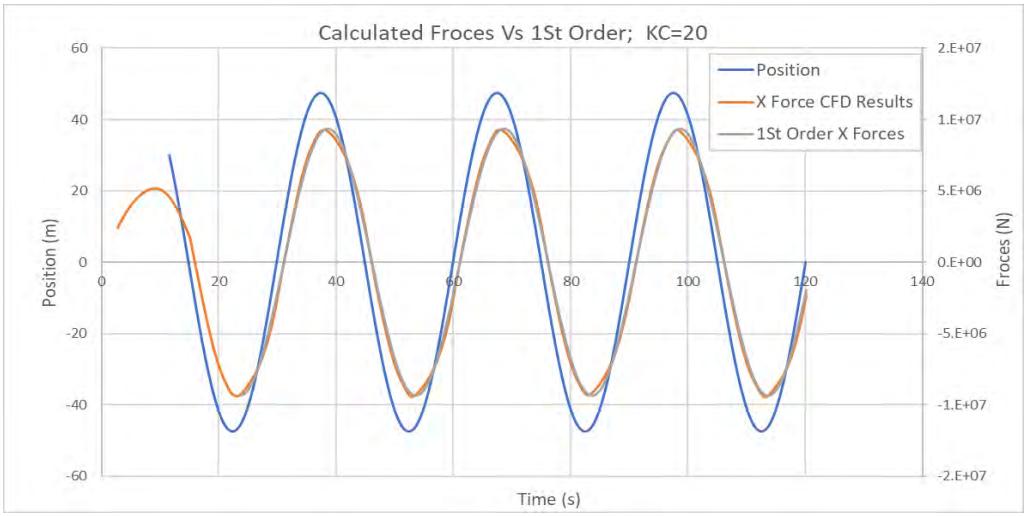

Figure 50: KC 20. CFD force Signal and 1st order fit

Figure 51: KC 20. Force Decomposition

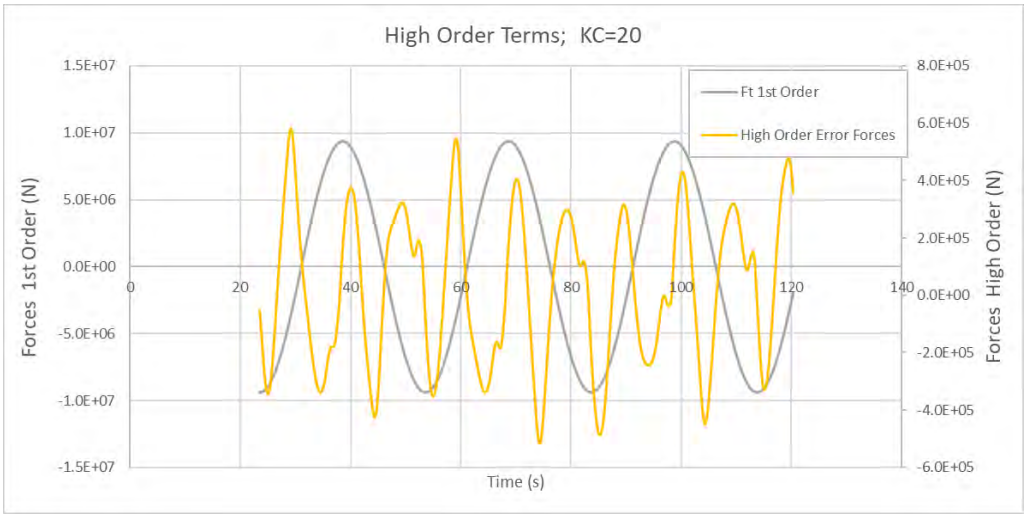

Figure 52: KC 20. 1st and Higher order terms (different scales)

Total Forces; KC=20	
Phase (deg)	-11.89
F total Amplitude 1s Order (N)	9.356E+06
F inertia amplitude (N)	9.155E+06
F viscous amplitude (N)	1.93E+06
Second Order Force Amplitude RMS (N)	2.81E+05
Mass (t)	3803.0
Added Mass (t)	606.1
Damping (kN/(m/s))	194.0

Table 29 : Result Example for Pontoon; KC 20

Section Forces; KC=20	HULL1 Fx	HULL2 Fx	HULL3 Fx	HULL4 Fx	HULL5 Fx	HULL bott
Phase (deg)	-9.87	-10.37	-11.30	-12.74	-12.34	-68.55
F total Amplitude 1s Order (N)	1.89E+06	1.88E+06	1.87E+06	1.86E+06	1.83E+06	1.18E+05
F inertia amplitude (N)	1.86E+06	1.85E+06	1.84E+06	1.81E+06	1.79E+06	4.33E+04
F viscous amplitude (N)	3.24E+05	3.23E+05	3.21E+05	3.19E+05	3.13E+05	2.03E+04
Mass (t)	760.6	760.6	760.6	760.6	760.6	0.0
Added Mass (t)	136.7	131.5	124.8	113.5	99.3	20.9
Damping (kN/(m/s))	32.6	32.5	32.4	32.1	31.5	2.0

Table 30 : Result Example for Pontoon Sections; KC 20

6.2 2D KC ITERATION SENSITIVITY.

7 ADDITIONAL 2D KC FLUID DOMAIN SENSITIVITY

A 2D slide of the 3D mesh used for 3D KC cases is generated with original fluid domain size: 250 x250m dimension.

Another 2D mesh with 500x500m dimension is generated. Near wall mesh size is identical in both mesh. Outer mesh size in the 500x500m domain is double to arrange a similar far field mesh size in both cases. So roughly 500x500m mesh is similar max element size as 250x250 size.

Case tested is KC1 Velocity amplitude 0.99m/s, roughness 1mm, 5 iterations, time step 0.25s.

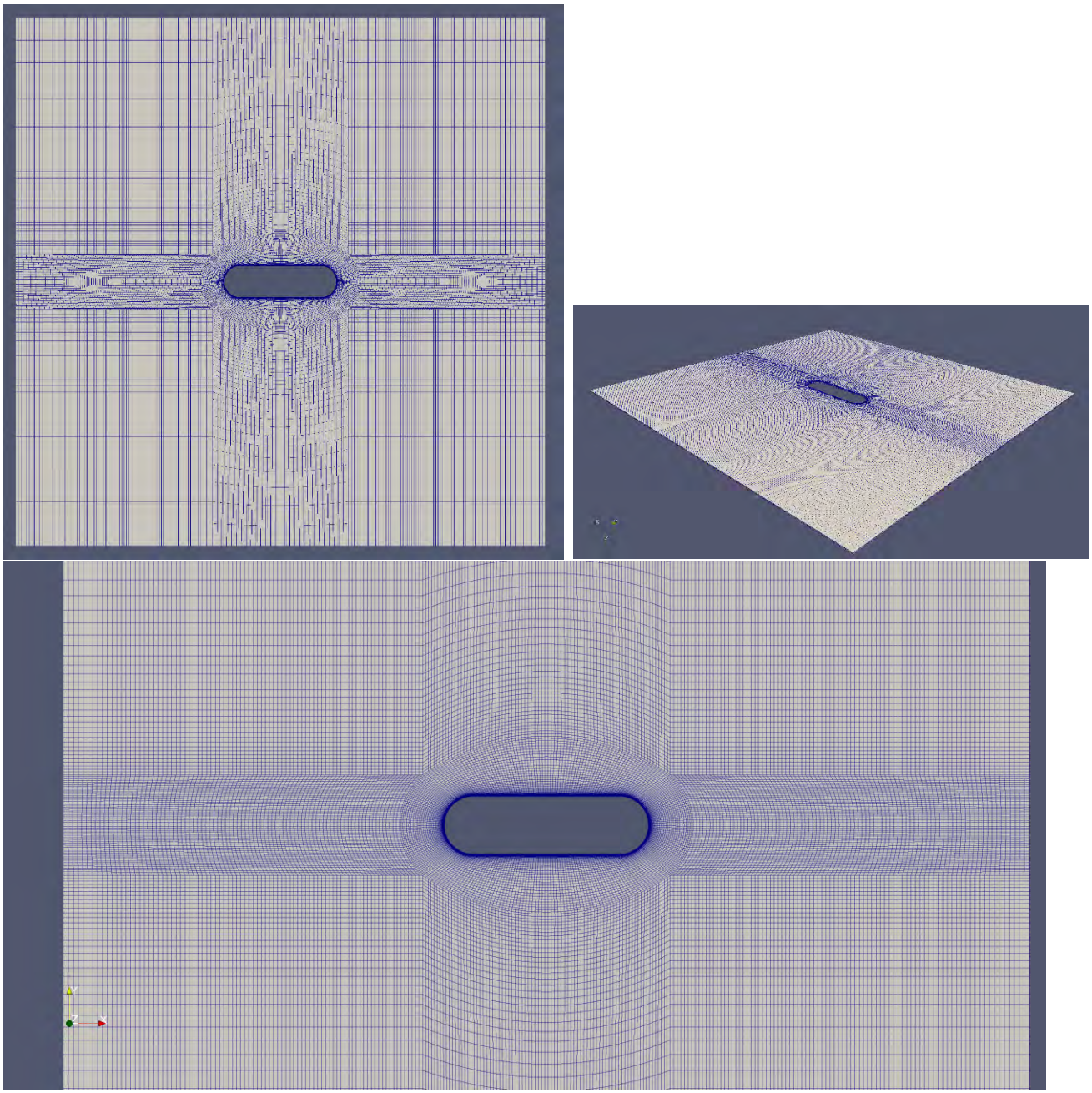

Figure 53 : Fluid Domain size Sensitivity results 2D, 250x250m mesh

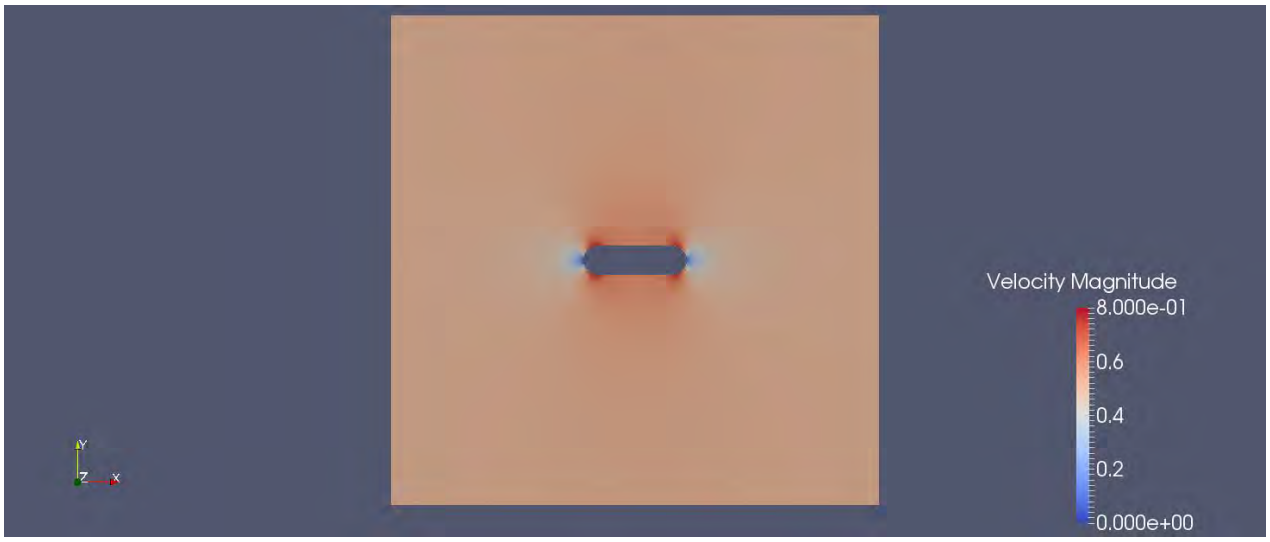

Figure 54 : Fluid Domain size Sensitivity results 2D, 250x250 mesh size, time step 400 KC1

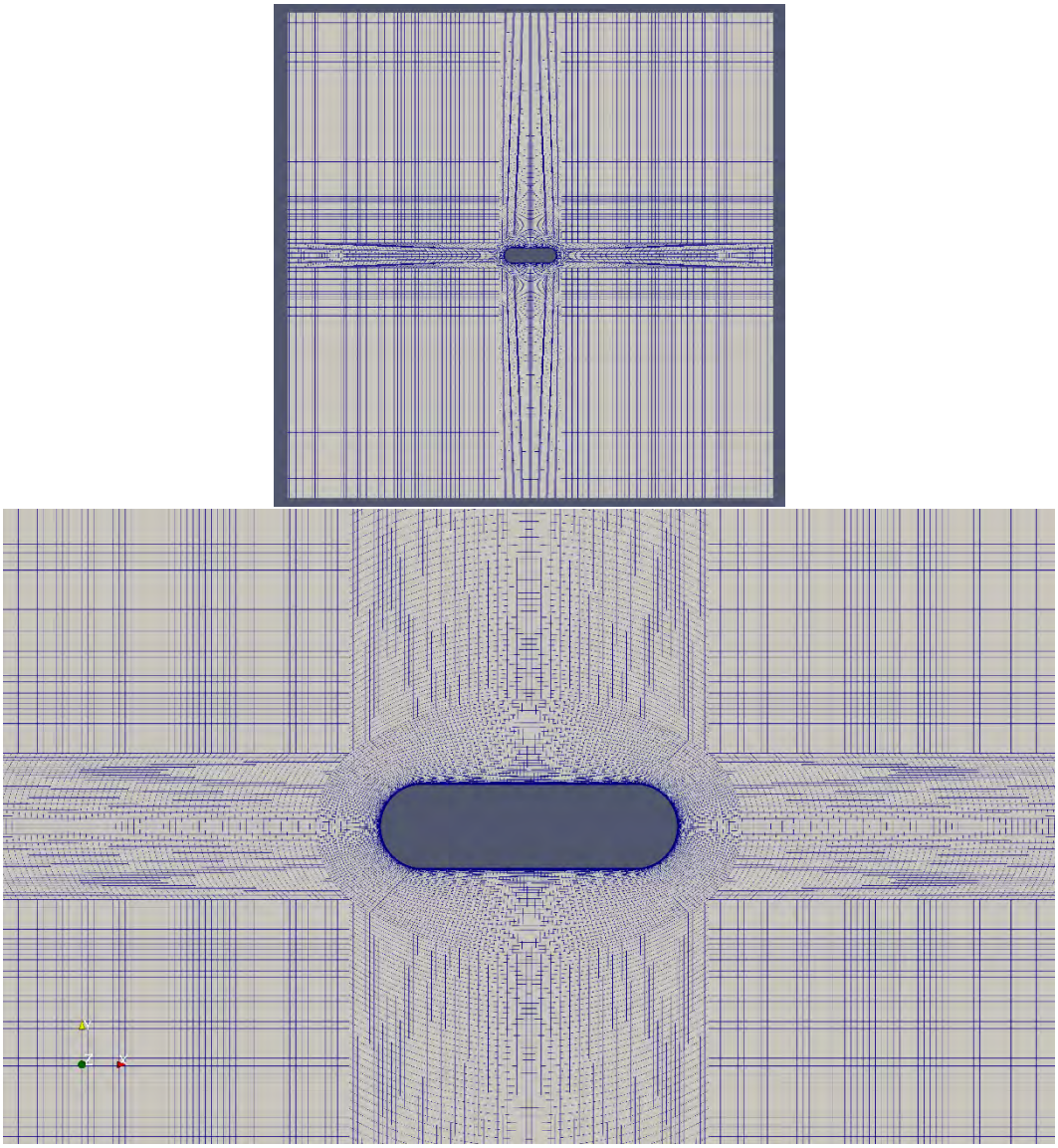

Figure 55 : Fluid Domain size Sensitivity results 2D, 500x500m mesh

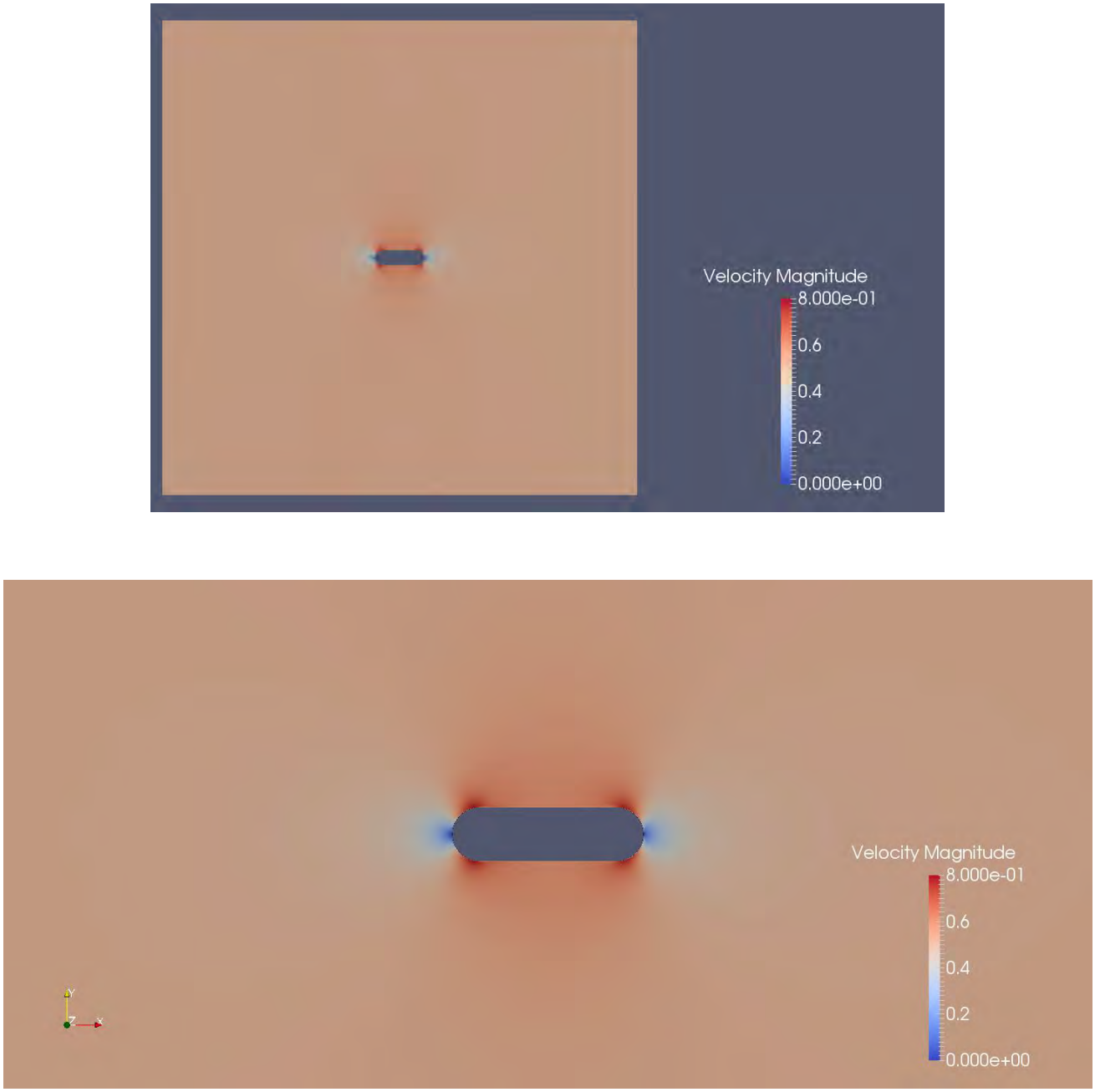

Figure 56 : Fluid Domain size Sensitivity results 2D, 500x500 mesh size, time step 400, KC1

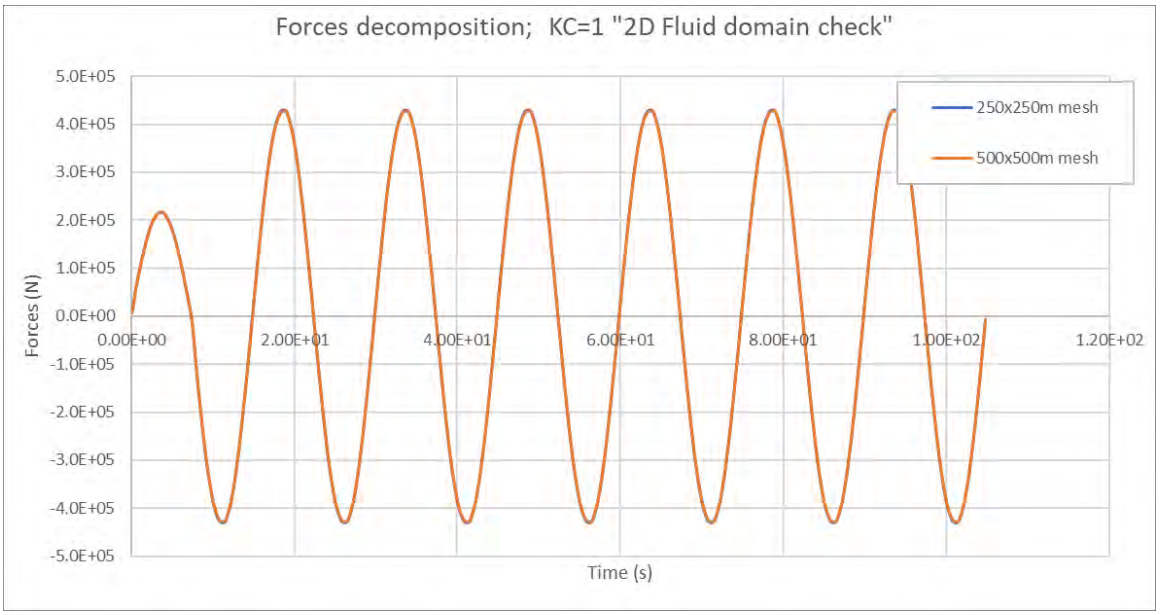

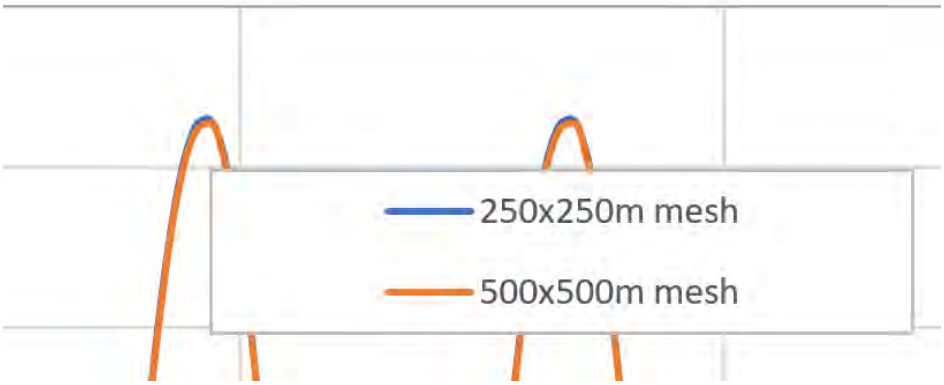

Difference in peak over two simulation: mesh 250x250 overpredict values compared with 500x500 mesh with a difference less than 1%. This value is considered acceptable.

8 REFERENCES

A. Iturrioz, R. G. (2015). Validation of OpenFOAM® for Oscillating Water Column three-dimensional modeling,. *Ocean Engineering*, Volume 107.

Brecht Devolder, P. R. (2017). Application of a buoyancy-modified k-ω SST turbulence model to simulate wave run-up around a monopile subjected to regular waves using OpenFOAM®,. *Coastal Engineering*, Volume 125.

Pablo Higuera, J. L. (2013). Simulating coastal engineering processes with OpenFOAM®,. *Coastal Engineering*, Vol 17.